Utrecht University

Master Thesis

Water Science and Management

Design and Construction of an Experimental Setup for BioSealing Application in Artificial Groundwater Recharge

Department of Earth Sciences

Environmental Hydrogeology Research Group

Corresponding author:

Giovanni Cecchetto S.

Supervisors:

Prof. Dr. Ruud Schotting

Dr. A Raoof

Abstract

Water is one of the most important drivers for human life and nature, and its availability often constitutes a limit on economic development and human welfare. Under a changing climate scenario, the variability of water supply is increasing while water demand is also expected to increase. Therefore, providing sufficient water supply at affordable rates will become one of the greatest challenges that humankind will face in the coming years. In fact, effective and innovative use of water resources has become one of the most active topics of research within the academia and the industry.

As a matter of fact, in the early 2000's, a novel geoengineering technique for a microbial sealing process was performed by Deltares (formerly GeoDelft) in the Netherlands, to reduce leakage flow through dikes. After four years of research Deltares patented a method called BioSealing, which consisted of the injection of nutrients into the soil to stimulate the growth of naturally present micro-organisms (bacterial growth) in the subsurface, in an anaerobic environment. The converging groundwater flow transports these nutrients towards a leaking structure, where the formed biomass induces clogging and reduces the flow rate passing through the leakage.

In this study, the BioSealing technique developed by Deltares is presented as an environmentally friendly technique that uses naturally present microorganisms to seal the subsurface, in order to accumulate water on top of fractured bedrock. As a first proof of concept for this novel technology, a laboratory setup was designed and constructed to demonstrate the efficiency of this process. The setup was built under different conditions in a sand-filled PVC tank, which contained a simulated leak in a water-retaining PVC layer with a 5cm gap in its centre. A water flow was pumped onto the topsoil of the tank, in a two-day trial to simulate an artificial recharge (AR) process within the sandbox, assessing then how the setup performed.

The AR simulation proved that the experimental setup is suitable to conduct a BioSealing experiment, being able to monitor the most important soil parameters —matric potential, dielectric permittivity, volumetric water content, bulk electrical conductivity and pore-water electrical conductivity— to study the clogging effect in time.

This study developed a first prototype to use the BioSealing technique as an alternative and useful geotechnical application, thus contributing to the solution of an important societal issue, such as recurrent droughts in times where climate change is compromising our water availability.

Keywords: BioSealing; artificial recharge; water tank experiment; 2D scale.

Content

List of Figures

List of Tables

1 Introduction

1.1 Background information

Global economic development coupled with climate change and continuing population growth is creating significant pressure on our global water resources. Indeed, times of water scarcity are now an inevitability for certain regions rather than a possibility (Intergovernmental Panel on Climate Change, 2019) and while water availability is drastically dropping, the competition for its use is intensifying (Ws & Wg, 2007). It is therefore evident that effective and innovative use of water resources will become one of the greatest challenges that humankind will face in the coming years and decades to achieve a sustainable economic development.

Besides, water is without doubt one of the most (if not the most) important driver for human life and nature and its availability often constitutes a limit on economic development and human welfare (Tarhule, 2017). In a changing climate scenario, the variability of water supply is increasing, whilst slightly reduced availability is projected (Organisation for Economic Co-operation and Development, 2016). At the same time, water demand is expected to increase, and providing sufficient water supply at affordable rates, while protecting water resources from depletion, will become more and more difficult (Ziolkowski & Ziolkowska, 2017). Additionally, many sectors, such as agriculture, mining and energy production, strongly compete for water resources availability. Thus, water scarcity compromises overall stability within regions and can cause instability in food prices, famine and even death in extreme cases (de Marsily, 2007).

A clear example is the province of China Yunnan, that has suffered frequent and severe droughts throughout history. In fact, as Li et al., (2019) points out, Yunnan experienced 21 severe droughts from 1961 to 2009. Furthermore, the authors' study depicts the consequences of a severe drought that hit this Province from autumn 2009 to spring 2010, threatening 25.12 million residents (55%), of which 7.57 million suffered from a lack of drinking water. The drought was so severe, that approximately 21,741 km2 of the crops planted between autumn and winter was affected, producing a total agricultural loss of around 20 billion renminbi (Lü et al., 2012).

However, according to Fan et al., (2013) the mean annual precipitation of Yunnan's whole region is about 1100 mm, of which 85% occurs in the wet season (from May to October). In contrast, according to the Royal Netherlands Meteorological Institute (KNMI), the average annual precipitation in the Netherlands ranges from about 700 to 900 mm a year, and this is already considered to be within rainy ranges, according to the KNMI.

Hence, the problem for Yunnan is that since most of the soil within this region is situated on top of fractured rock (Li et al., 2019), the infiltration from rainfall events is transported by gravity downwards through the unsaturated zone, and finally drained by the fractures in the underlying rock formations. This explains why hardly any groundwater tables can be found in the topsoil in Yunnan. Accordingly, most of the rainwater in the region is lost through deep infiltration and stored in fractured rocks, sometimes as deep as 150 meters below ground level. Water extraction in these conditions is extremely expensive due the machinery and the energy needed, and given the economic situation in Yunnan, drilling to these depths through bedrocks is no option.

As an integral part of its Corporate social responsibility (CSR) program, the Public Advice International Foundation (PA International) arranged an expert mission to Yunnan. The expertise of the invited scientists was diverse: water management (hydrogeology), bamboo science, irrigation, food production and enrichment, hydrology and hydromechanics, etc. The aim of the mission was to expose these scientists to the actual situation in Yunnan and inspire them to come up with possible solutions contributing to a 'drought-preparedness plan' for Yunnan.

Soil erosion in Yunnan is recognized as a major environmental and economic problem (Whitmore et al., 1994). Especially during rainy season, the erosion of the topsoil layer is extreme, since the plains used for agriculture, industry and urban growth have outreached towards steep slopes and marginal lands, accelerating erosion rates during seasonal rainfall events (Barton et al., 2004). Consequently, the surface runoff is highly concentrated with sediment, converting the waterflow from streams and rivers into a brownish-yellow and highly viscous fluid. This phenomenon can be explained by the presence of highly dense crop fields in the topsoil layer, of which maize occupies 23% of the total cropping area (Barton et al., 2004). Maize is often grown on infertile land, with low water content and a very high runoff ratio because of the steep slopes combined with a high catchment discharge. Maize and crop presence perturbate the structure of the soil, making it less compact, which in turn makes the terrain vulnerable to runoff erosions during the rainy season.

Unfortunately, the aforementioned situation does not only affect the province of Yunnan in China, but can also be found everywhere else in the world, where long periods of drought are followed by short intensive rain events, in Chile for instance, where 25% of the country is affected by soil erosion and more than 60% of the total usable land is already degraded (Ellies, 2000). Then, the main problem is how to control soil degradation produced by rainwater and runoff, considering that in water scarce areas, non-natural capacity (reservoirs, lakes etc.) can store only a limited amount of freshwater. Drinking water demand in densely populated dryland areas can barely be met nowadays, and in combination with the need for irrigation and cattle, freshwater demand is almost impossible to supply in those areas. Therefore, it is urgent to find alternative methods to supply freshwater to densely populated dryland areas, such as Yunnan or Chile, to ensure enough water for their livelihood, agriculture and livestock.

Within PA International's mission the idea that stood out was to naturally clog, and seal the fractures within the bedrocks, so that water could be stored in the soil layer overlying the fractured rock. Then, a water table can be created at a shallow and far more reachable depth and the soil layer can be recharged during the rainy season. Some engineering techniques to naturally clog the soil have already been already developed by several authors (Admiraal & Molendijk, 2006; Blauw et al., 2009; Charbonneau et al., 2006; Liao et al., 2007; Ross, 2004; Ross et al., 2007; Ross & Bickerton, 2002; van Beek, 2007; van Paassen, 2011; Weersma et al., 2005; W.O. Molendijk, W.H. van der Zon, G.A.M. van Meurs, 2009) and their research was accomplished by stimulating the growth of naturally occurring bacteria present in the soil and groundwater. The principle of the process is to stimulate the biological activity of micro-organisms present in the soil by adding nutrients that will accelerate the bacterial growth and create biomass. Once sufficient biomass is formed, a convergent groundwater flow in the porous medium towards the fracture is injected to induce a natural clogging process.

This process gained recognition when Deltares (formerly known as GeoDelft) developed the concept of SmartSoils®, a research program that aimed to develop novel geoengineering techniques by changing soil properties (e.g. permeability, stiffness, strength) to fulfil pre-specified requirements for construction activities. In 2005, under the SmartSoils programme, Deltares conducted a field experiment implementing a novel technique called BioSealing, which proved to be able to stop the leakages in water-retaining civil constructions like sheet pile walls and earth dams (Blauw et al., 2009). It was the first geoengineering technique successfully applied in a series of field tests experiments throughout the world (e.g. in the Netherlands, Canada, Austria) in different kinds of engineering applications.

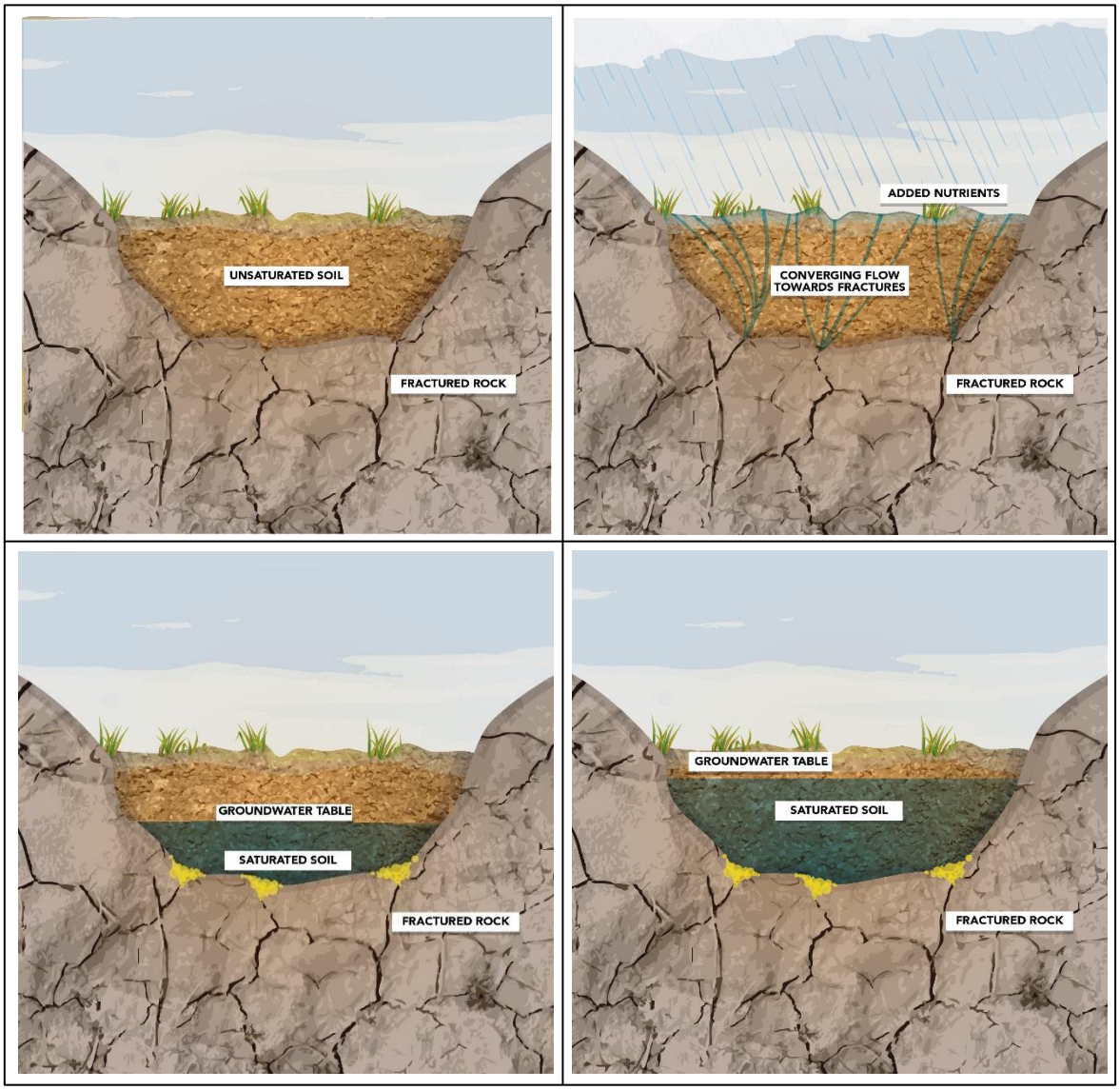

Figure 1-1: Sequential image of the ideal field experiment

Over almost fifteen years of investigation, BioSealing proved to be an effective geoengineering technique mostly used for sealing small-scale water-retaining constructions, as well as preventing migration of pollutants out of contaminant-retaining structures both at the surface and subsurface. Nonetheless, there is still no evidence of BioSealing use in any other type of civil engineering application at a larger scale. This research will be focused on doing so, by using this technology with the purpose of constructing artificial

(man-made) aquifers. To that end, a laboratory environment will be designed and constructed in order to prove that this technique is also suitable for changing the water content (θ) of the soil, enhancing the water distribution and porosity of a soil-column. This will be the first approach for a further implementation phase at a larger scale, that will aim at improving soil conditions in a specific area affected by drought (to be defined: Indonesia, Oman, China, The Netherlands, Chile, etc.).

Figure 1-1 depicts a sequential process of the ideal field experiment and second phase of this study. The upper-left image shows no freshwater present in the subsurface since, in natural conditions, the surface runoff and superficial freshwater available for recharge vanishes into the fractures and no groundwater table is formed. The upper-right image shows the application of nutrients on the overlaying soil, infiltrating to the subsurface (together with the surface runoff or though injection wells installed in the subsurface) and transported by a converging flow towards the fractured bedrock. The bottom-left image shows how the fracture's throats are sealed due to biomass formation at its position; this process, in turn, induces a mechanical clogging in the fracture and a thin groundwater body is appreciated. Finally, in the bottom-right image, the aquifer is charged during rainy seasons, such that a groundwater reservoir is formed, providing water availability for future use during eventual periods of (severe) droughts.

1.2 Objective

As a first stage of this project, the Environmental Hydrogeology Group at Utrecht University needs to develop a laboratory prototype for BioSealing application as an appropriate technique in artificial groundwater recharge. Therefore, the main goal of this study is to build an experimental setup as a proof of concept of this novel technology. This work will complete the first laboratory phase of the project to reach a component and/or breadboard validation in a laboratory environment.

Then, the main research question to be answered is:

How to implement a laboratory environment to assess whether the application of the BioSealing technique is feasible in artificial groundwater recharge applications?

2 Theoretical framework

2.1 BioSealing applications

In the beginning of the 21st century, a novel geoengineering technique for a self-searching microbial sealing process was performed both in the Netherlands and Canada. In the Netherlands the research aimed at stimulating microbial activity to reduce leakage flow through dikes, thus preventing damages near leaking underground water-retaining constructions; whereas in Canada the aim was to limit spreading of polluted groundwater in limestone and soil remediation by enhanced biodegradation (Lambert et al., 2010).

In 1999, Deltares (formerly GeoDelft and one of the most important Dutch research institute for ground and superficial water issues), started a research project in collaboration with contractor Volker Wessels and Delft University of Technology. The project developed biological methods for sealing water-retaining engineering structures (van Paassen, 2011). Within this project, a novel geoengineering technique was introduced, in which they stimulated the natural clogging process that usually takes place in the vicinity of groundwater wells, at the subsurface. After four years of experiments, Deltares patented a method called BioSealing, which consisted in the injection of nutrients at various places and various depths of the soil column in order to stimulate the growth of naturally present micro-organisms (bacterial growth) in the subsoil, in an anaerobic environment. Then, converging groundwater flow transports these nutrients towards a leaking structure, where the formed biomass induces clogging and reduces the flow rate passing through the leakage (Weersma et al., 2005).

Several laboratory experiments were conducted (Ross et al. 2001, Van Beek et al. 2007, Veenbergen et al., 2005), but the most remarkable one was done in 2006, where a PVC column was filled with natural Dutch Pleistocene sand and, to simulate seepage, an impermeable disk with a centred leakage hole of 4 cm diameter was inserted in the column. A constant head difference was applied over the column, by a separate storage tank with a higher water level than the test column, causing thus a constant pressure flow (Admiraal et al. 2006). To stimulate bacterial growth, potato starch was injected to the column. The injected substrate was Nutrolase, which is a mineral-rich product from the potato that is added to compound feed - for example as a molasses substitute. produced and distributed by AVEBE. In this experiment, conductivity, pH, temperature, oxygen concentration and redox potential were monitored, and the clogging factor was calculated, by equation (2.1).

From these series of experiments, the most important result was the observation of a decrease in permeability with a clogging factor of 5 to 20 and even total plugging of columns after adding Nutrolase. It was also found that even after stopping the nutrition supply, the clogging effect produced by the bacteria stayed stable for the duration of the test, which was up to 4 months in some cases (Admiraal et al. 2006).

As an upscaling of the laboratory trial, a first field experiment was executed by Deltares in 2004, near the port area of Rotterdam, "*the Maasvlakte*". In this research, the water demand to maintain a certain water level in the container decreased with a factor of 5 and eventually by a factor of 30 after four weeks (van Paassen, 2011). The process was monitored measuring both phreatic level and the quality of the groundwater. In this experiment it was found that the plugging not only occurs near the leaking gap, but already starting from the point of injection. However, clogging in the soil is most intense near the leakage.

In this field experiment it was also found that after 3 months the clogging effect was still in existence and a reduction in the flow rate was measured with a factor varying from 12 to 28 (Admiraal et al. 2006).

It is important to highlight that in this experiment, the drain for the effluent flow was constructed in a gravel filter in order to avoid clogging in the vicinity of the outlet. This is because, the circumstances nearby the drain are similar to those nearby the leak: streamlines come together, and the flow rate increases. It is therefore not unrealistic that when the permeability nearby the leakage reduces, this also happens nearby the drain, which is an unwanted side effect. The large porosity of the gravel filter is there to avoid this potential problem of clogging.

Another BioSealing pilot study was performed in 2007, where a joint venture between VERBUND (leading Austrian Energy company), Insond (ground engineering specialist, subsidiary of Züblin Spezialtiefbau GmbH) and Deltares developed a possible solution for seepage reduction, to seal leakages in levees along the Danube in Austria (Lambert et al, 2010). In this research it was found that the discharge started to decrease sufficiently after 10-12 weeks. Indeed, a decrease in discharge is measured with a factor of 7.4 from 17.33 m^3/day to 2.35 m^3/day. The clogging factor at the leaking location was estimated to be 10 (Blauw et al., 2009).

A few years ago (2015), Deltares launched a Joint Industry Projects (JIP), together with Sireg (Italy), Zuckerforschung Tulln (Austria), Bioclear (the Netherlands), Texplor (Benelux), Avebe (the Netherlands), Züblin Spezialtiefbau (Austria), Volker Staal en Funderingen (the Netherlands) and GEOtest (Czech Republic). The projects were done both in Czech Republic and the Netherlands. The BioSealing technique was applied at the Hornice dam, which is a water reservoir in located in Czech Republic, southwest of the City of Brno. The process of sealing the dam with bacterial growth was documented in time by measuring water levels in the reservoir, seepage discharge, as well as the changes in the electrical conductance of the dam soil using the method of electrical impedance spectroscopy (EIS) (Paílková et al., 2017).

It is also important to highlight the work done in 2002 by Nathalie Ross in Canada, which proved that with biostimulation natural bacteria could generate a biofilm as thick as 1,100 μm in a ceramic surface. Furthermore, Ross and Bickerton (2002) showed that bacterial populations clogged a single limestone fracture up to 99.2 percent after 22 days. In their fieldwork, the generated biobarrier resulted in a five time decrease of the hydraulic conductivity in the fractured bedrock, after only 2.5 days of biostimulation. Moreover, after injecting 65,000 gallons of molasses and nitrate in 11 wells positioned in a centreline perpendicular to the flow direction, the bioaugmentation decreased K by 99.4 percent.

From the applications described in the paragraphs above, it can be concluded that the BioSealing technique has been widely used in engineering applications to reduce the flow through water retaining constructions or natural non-porous layers as well as prevention of contaminants through Fractured Bedrock Sites (Ross & Bickerton, 2002), but no study was found related to water availability.

Several experimental analysis and laboratory tests have been carried out to study the influence of the different nutrition, minerals, concentrations, catalysts, temperature and scale. (Admiraal & Molendijk, 2006). And one important finding for the purpose of this research can be found in Weersma et al. (2005), which investigated the injection of three types of nutrition: Syrup (treacle), Solvicol (hard decomposable

starch), and Nutrolase (simple decomposable protein). In this experiment they found out that with the latter type, the clogging starts with biomass and it is then reinforced by a (biologically induced) chemical precipitation of iron sulphide. Therefore, they claimed that the best outcomes were achieved with Nutrolase, a residue of the production of potato starch that so far has been unharmful to the environment.

2.2 Detection techniques

As shown before, several experimental results have proved that BioSealing is an effective way to reduce the seepage discharge, decreasing soil permeability. However, it is difficult to conclude that the plugging effect was caused due to the biomass growth and stimulation of bacteria since they are impossible to detect in-situ, without intervening or disturbing the natural soil/water/air matrix. That is why, over time, , several detection techniques have been developed by engineers and development teams in charge, to monitor the BioSealing formation. In this section, the most important and relevant techniques will be reviewed.

2.2.1 Clogging Factor

One of the most used methods in the field experiments that were carried out in the Netherlands is the measuring of the clogging factor with equation 2.1:

$$C_i = \frac{\left(\frac{\Delta Q}{\Delta h_i}\right)_{t=0}}{\left(\frac{\Delta Q}{\Delta h_i}\right)_{t=t}} \qquad 2.1$$

where ΔQ is the decline in flow; and Δh is difference in head between 2 manometers. At the start of the monitoring, C is equal to 1 and by decreasing permeability or difference in groundwater level C will increase (Veenbergen et al., 2005).

2.2.2 Flow differences

It is intuitive and self-explanatory that a decreasing effluent flow indicates a decreasing permeability nearby the leak. To estimate this flow reduction, the difference between the inlet flow and the outlet flow can be estimated by measuring both flowrates in time. For instance, in the experiment done at the Hornice dam, the main monitored parameter used to assess the BioSealing effectiveness was the seepage, which was measured by a PF500 shuttle tilt flowmeter (Paílková et al., 2017).

2.2.3 Physicochemical properties

Normally, chemical properties of the groundwater, such as pH, electrical conductivity (EC), pore-water EC, oxygen and redox potential (decreasing in redox potential indicates an increasing micro-organism activity) are monitored throughout the whole BioSealing application (Veenbergen et al., 2005). These parameters can be used to compare the influent with the effluent, assessing the changes related to biomass formations (Pazdírek, O., 2017). However, physical properties, such as the water temperature for instance, are not as accurate as the clogging factor or flow difference to determine how effective the clogging effect was in the sealing process. Therefore, physicochemical properties are recommended as a third or additional parameter to study the clogging effectiveness.

3 Materials and methods

This chapter will introduce the materials and methodological approach utilised during this research project. The experimental set-up will be outlined, specific materials and equipment introduced and justified, and the model background detailed.

3.1 Experimental setup

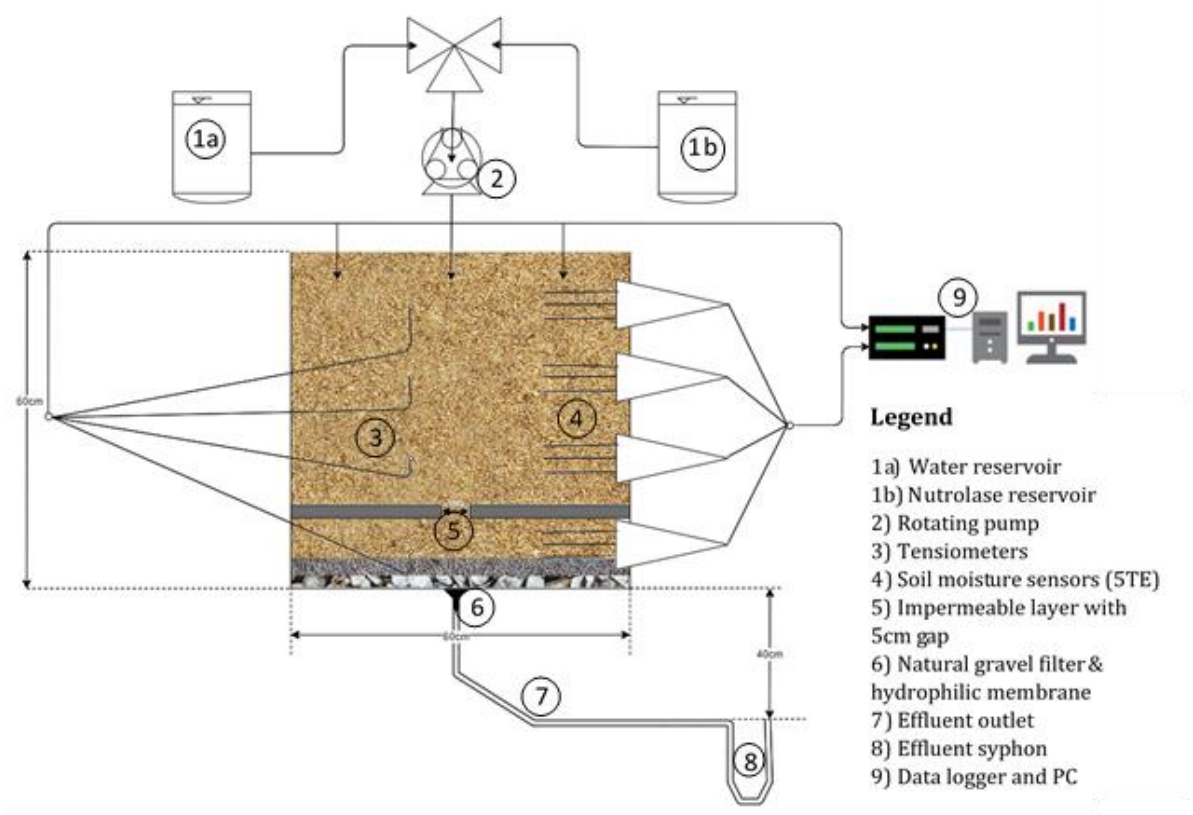

Figure 3-1: Schematic design of the experimental setup

On both sides of the 60-cm-long tank, sensors are installed. The sensors on the right side of the column are soil moisture sensors (5TE) and the sensors on the left are tensiometers [Rhizo Instruments (Wageningen)]. The tensiometers measure the pressure head at equidistant depth (z=-5, -20, -35, and -46,5 cm) along the column. The 5TE sensors are inserted at equidistant depth equal to the depth of the tensiometers. Both tensiometers and 5TE-sensors are directly transmitting electrical data to the datalogger. The 5TE sensors measure the soil bulk dielectric permittivity (ε), the bulk electrical conductivity (σ_p) and temperature (T).

At the height of 10cm, a water-retaining PVC layer with a 5cm gap in its centre. was installed to simulate a leak in a fractured bedrock.

On the bottom, the tank was fitted with a 3-part coupling with 2 internal adhesive connections and a diameter of 75 mm. A hydrophilic membrane was installed on the outlet to prevent air from entering the setup. The outlet was finally connected to a tube with a syphon shape, and a water level of approximate 40cm below the outlet. This syphon applies a negative pressure (relative to atmospheric) to the tank, simulating

unsaturated conditions. The hydraulic gradient is constant, maintaining a height difference of 40 cm between the outlet and the top part of the syphon.

A gravel filter was also installed in the bottom drainage to prevent the plugging of the effluent outlet.

3.2 Materials & measuring equipment

3.2.1 Sand material

The sand was obtained from Griftpark, Utrecht. The type of soil present at Griftpark consists of an impermeable clay layer, contained by a concrete wall of about 50 meters deep and 1,235 meters long, topped by a blended 1.5-meter cap of lining, sand and topsoil (Marlet, 1999). The sand was collected from the topsoil which is known to have bacterial population.

After collecting the soil samples, the sand was cleaned and filtered with a 4mm Garland Fine-meshed Seed Sieve and in some cases a 200 dia. x 25mmH RETSCH Stainless Steel Test Sieve before usage. A hyprop experiment was conducted in order to obtain the most important physical properties and hydraulic parameters of the soil sample. The soil water retention curve (SWRC) was also calculated with Hyprop to illustrate the relationship between soil water content and soil water potential of a small portion of soil.

Gradation test and Thermogravimetric (TGA) analysis were also performed to study the grain size distribution as well as the Organic Material (OM) composition of the soil. The obtained parameters are shown in Table 3-1.

Table 3-1: Soil properties

Property	Value
D50 - mean particle diameter [mm]	0,33
D [3, 2] - Surface weighted mean [-]	0,16
D [4, 3] - Volume weighted mean [-]	0,42
ρ_b^d – dry bulk density [g*cm^{-3}]	1.61
ρ_s – density of solid substance [g*cm^3]	2.65
K_s - saturated conductivity [cm*h^{-1}]	0,017
φ - average porosity [-]	0,39
Organic matter content	7%

3.2.2 Tensiometers

The tensiometers (Figure 3-2) were used to measure the matric potential (ψ) or suction in the soil at four different depths in the tank (z=45, 30, 15 and 5 cm).

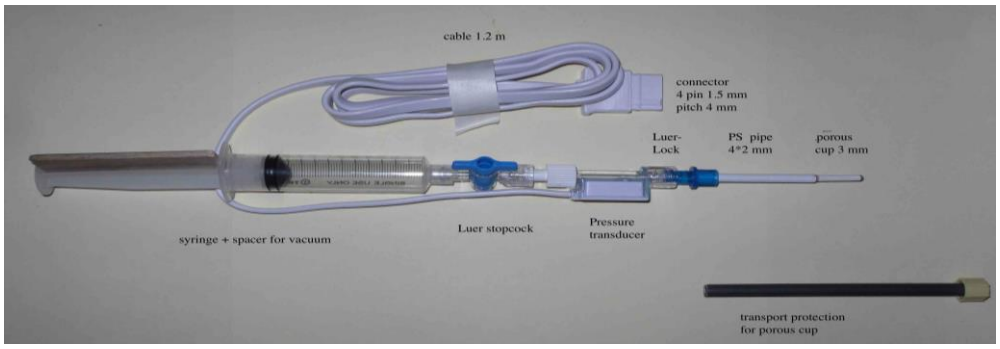

Figure 3-2: Autofill tensiometer (Rhizo Instruments)

A permeable cup allows the water present in the pores of the soil to enter through a PS pipe. The tension between the water-tube and the soil is always in equilibrium when no flow is occurring. Thus, the potential in the tensiometer tube is equal to the potential in the tank, and this pressure is measured relative to suction pressure in the syringe. The syringe has a vacuum chamber of 10ml space, which is close to a pressure of -1 atmosphere, meaning that the pore suction pressure in the shaft is also near -1 atm. Finally, the relative matric potential is measured by the pressure transducer in the middle of the shaft, which sends an electrical signal in voltages to the datalogger, that converts this signal into cmH_2O and records the tension value every 5 minutes. The tensiometers were inserted horizontally at the centre of the sandbox, to maintain the pressure transducer at the same height of the measured potential, giving thus more accurate results.

3.2.3 5TE soil moisture sensors

The 5TE soil moisture sensors (Figure 3-3) are designed to measure the volumetric water content (VWC), Electrical Conductivity (EC), and temperature (T) of the soil. To determine the water content these sensors use an oscillator running at 70 MHz to measure the dielectric permittivity constant of the surrounding soil (ε). They are also equipped with a thermistor that in thermal contact with the sensor prongs provides the soil temperature. However, for the purpose of this experiment the differential values of the temperature are neglected due to very small differences in the laboratory environment.

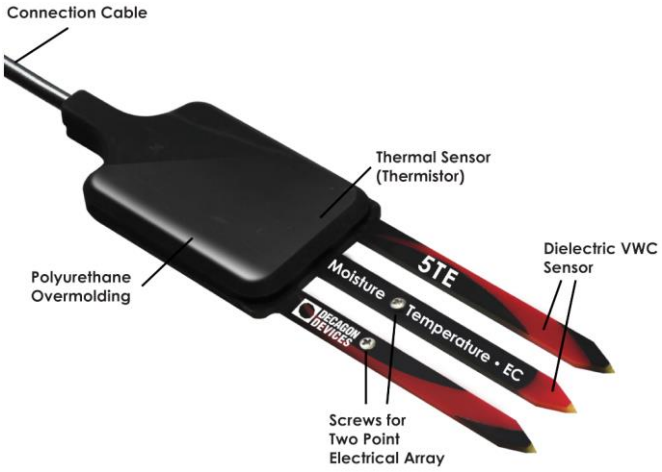

Figure 3-3: 5TE-sensor and components (Decagon Devices, 2016).

3.2.3.1 Volumetric Water Content (VWC)

To estimate the VWC the 5TEs measure the dielectric constant or relative permittivity of the surrounding medium through an electromagnetic field. The prongs supply a 70 MHz oscillating wave to the sensor that charges according to the dielectric of the material. Each material has different dielectric constant values and a material with high permittivity polarizes more in response to an applied electric field than a material with low permittivity, thereby storing more energy in the material, e.g., air has a relative permittivity of 1, whereas soil and porous materials ranges between 2 and 5. The relative permittivity for liquid water is around 80, which means that water has a higher ability to store charge than other materials. On the contrary, air has almost no storage capacity for electricity, whilst other materials present in the soil are always constant.

Specifically, the 5TE microprocessor measures the charge and outputs a value of dielectric permittivity from the sensor. Then, the dielectric permittivity data retrieved from the 5TE is converted into VWC with the Topp equation (3.1) (Metergroup, 2018).

$$\theta = 4.3 * 10^{-6} * \varepsilon^3 - 5.5 * 10^{-4} * \varepsilon^2 + 2.92 * 10^{-2} * \varepsilon - 5.3 * 10^{-2} \quad 3.1$$

3.2.3.2 Electrical Conductivity

Electrical Conductivity is defined as "*the ability of a substance to conduct electricity*" (Metergroup, 2018) and this value can also be used to infer the number of charged molecules present in a specific solution. The 5TE sensors are equipped with a two-electrode array to measure the bulk EC of the surrounding medium. To measure the EC throughout the soil, alternating electrical current in two electrodes are applied and the resistance between them is measured, estimating thus the soil resistance (R). The bulk EC is then derived by multiplying the inverse of the soil resistance (R^{-1}=G=conductance) by the ratio of the distance between the electrodes to their area (cell constant).

5TE bulk EC measurements have an accuracy of 10% in ranges between 0 and 7 dS/m. However, some special soil applications may require measurements with bulk EC greater than the specified range, for instance salt-affected soils or nutrolase in this case. This happens because the different properties of the porous medium and gases, liquids or chemicals compounds present in the pores have also influence the soil EC. Therefore, the bulk EC is influenced by the type of porous medium (sand, loam, clay, etc.), moisture content (θ), gas content (i.e. air) and solute concentration (nutrolase for instance). According to the manufacturer, the 5TE sensors can measure up to 23.1 dS/m bulk EC and above 7 dS/m, requires user calibration (see **Appendix D**).

3.2.3.3 Pore-water electrical conductivity

For many soil and water applications, it is valuable to know the EC of the solution contained in the soil pores (σ_p), as it serves as a good indicator of the amount of solute present in the soil. Traditional research methods involve invasive techniques that disrupt the experimental setup. These are usually performed by means of pore-water sampling, to obtain the water directly from the studied soil to measure the σ_p. However, this kind of procedure is a labour-intensive process and when not performed correctly it may also alter end results by changes made to the original conditions of the experimental setup.

METERGROUP (2018) developed an innovative way of calculating the pore-water EC, after several years of empirical research that helped finding a relationship between σ_b and σ_p. This relationship was found following the work done by Hilhorst (2000), in which he defines a linear relationship between the soil bulk dielectric permittivity (ε_b) and bulk EC (σ_b). Using this association, an accurate conversion from σ_b to σ_p is possible when ε_b is also known. The 5TE use Hilhorst (2000) equation to estimate σ_p, measuring ε_b and σ_b nearly simultaneously in the same soil volume:

$$\sigma_p = \frac{\varepsilon_p \sigma_b}{\varepsilon_b - \varepsilon_{b0}} \quad 3.2$$

where:

σ_p = pore-water electrical conductivity (dS/m);

ε_p = dielectric permittivity portion of the soil pore water (unitless);

σ_b = bulk EC (dS/m);

ε_b = dielectric permittivity portion of the bulk soil (unitless);

ε_{b0} = dielectric permittivity portion of the soil when $\sigma_b = 0$ (unitless);

Then, ε_p can be calculated from soil moisture using equation 3.3 (Metergroup, 2018):

$$\varepsilon_p = 80{,}3 - 0{,}37(T_{soil} - 20) \quad 3.3$$

Empirical research has shown that there is a linear relationship between the soil bulk dielectric permittivity and the bulk EC, as seen in Equation 3.33.3 , allowing an accurate conversion from bulk to pore-water EC (Hilhorst, 2000). Pore-water EC values were used in the experiment, to determine the concentration of nutrolase within the soil.

METER indicates that Hilhorst (2000) method results in good accuracy (20%) in most soils and porous media. However, since the measured permittivity is also influenced by the concentration of the solutes present in the soil, in some cases the linear relationship between ε_b and σ_b is not valid anymore. Indeed, in dry soils, where VWC is below 10%, the term ε_b-ε_{b0} becomes almost zero, leading to potential errors. Therefore, bulk EC should be used instead.

In the column experiment performed by de Witte (2017) a linear relationship was found between the concentration of the solute and the bulk EC, meaning that bulk EC (σ_b) was directly proportional to the solute concentration (C). The calibration curves developed by de Witte (2017), showed that the linear relationship between σ_b and C was true for different saturations. This relationship was described with Equation 3.4, as follows:

$$C(x,t) = A0\ ECb\ (x,t) + B0 \quad 3.4$$

where A0 and B0 are constants given by the slope of the curve and the intersection with the y-axis respectively.

Equation 3.4 only holds assuming that the water content is kept under unit gradient conditions, i.e. constant water content over time. However, for this experimental study, the water is changed over time, creating a high uncertainty in the system.

3.2.4 HYPROP

The relationship between the water content, θ, and the soil water potential, ψ, is very important in order to understand the behaviour of fluids and solutes during unsaturated conditions. This relationship has been very well studied by researchers and thanks to the scientific findings, more recently a new methodology has been developed by METERGROUP, (former UMS, Germany).

HYPROP (HYdraulic PROPerty analyser) is a technique to measure hydraulic key functions of soil samples in a simple and reliable way. The measuring procedure is based on G.P. Wind's evaporation method (Bezerra-Coelho et al., 2018). With this methodology, the water retention curve —relationship between water tension and water content or pF/WC— and the unsaturated hydraulic conductivity —relationship between Ks and θ—be measured at the same time, by combining the changes in mass and matric potential of a specific soil sample. The measuring time ranges between 2 days (for clay soils) to 10 days max (peat and sandy soils).

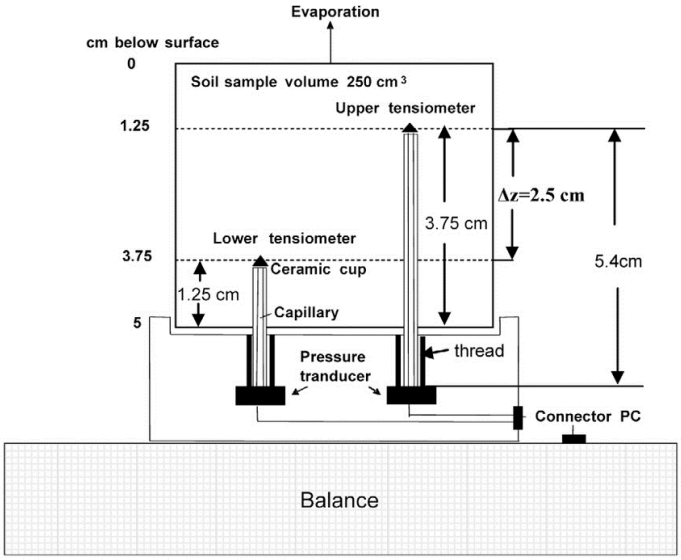

Figure 3-4: Schematic design of the HYPROP analysis (Bezerra-Coelho et al., 2018, after Schindler et al., 2010a)

Figure 3-4 shows a schematic design of the HYPROP empirical method and the different components of the experimental setup. The procedure for retention data determination is done by first packing the porous media in a 250 cm^3 stainless steel soil ring and flattening it with a blade at the top and bottom parts. The sample is then covered by a nonwoven cloth on the bottom and a plastic cap is placed on top. The soil core is then saturated by leaving the soil sample for a few days, in a container filled with DI-water. While the soil sample is being filled with water, two tensiometers are degassed and saturated to insert them at two different positions in the sensor unit (also saturated). The soil sample is then placed in a sample ring in the middle, between the two tensiometers, where an identical and symmetrical space is open to fix the core column onto the balance. The topsoil is then opened to the atmosphere so that the water can evaporate through the soil. HYPROP measures the weight loss due evaporation over time, while the average pF (water tension) values of the sample are determined based on the readings of the two vertical tensiometers shafts at different depths. The moisture content (θ) in the soil is also calculated based on the difference between

the dry and wet mass of the weighted sample. Both the change in mass and the matric potential are used to construct a single measuring value per point in time for the Soil Water Retention Curve (SWRC).

Finally, the measured retention data is fitted with van Genuchten (1980) using the integrated HYPROP-FIT software-:

$$\theta(h) = \theta r \frac{\theta s - \theta r}{[1 + |\alpha * h|^n]^m} \quad 3.5$$

Where:

Θ = VWC as a function of ψ;

Θr = residual VWC;

Θs = saturated VWC;

h = matric suction (ψ);

n, m = van Genuchten parameters.

Additionally, HYPROP determines the average porosity (φ) and the dry bulk density (ρ) of the soil sample, by calculating the masses and volume

3.3 Data analysis

3.3.1 Soil Organic Matter (SOM)

Two samples were taken to study the soil organic matter (SOM) content. A thermogravimetric (TGA) analysis (TGA) was conducted to each one of them, to calculate the percentage of organic matter (OM) present in the soil.

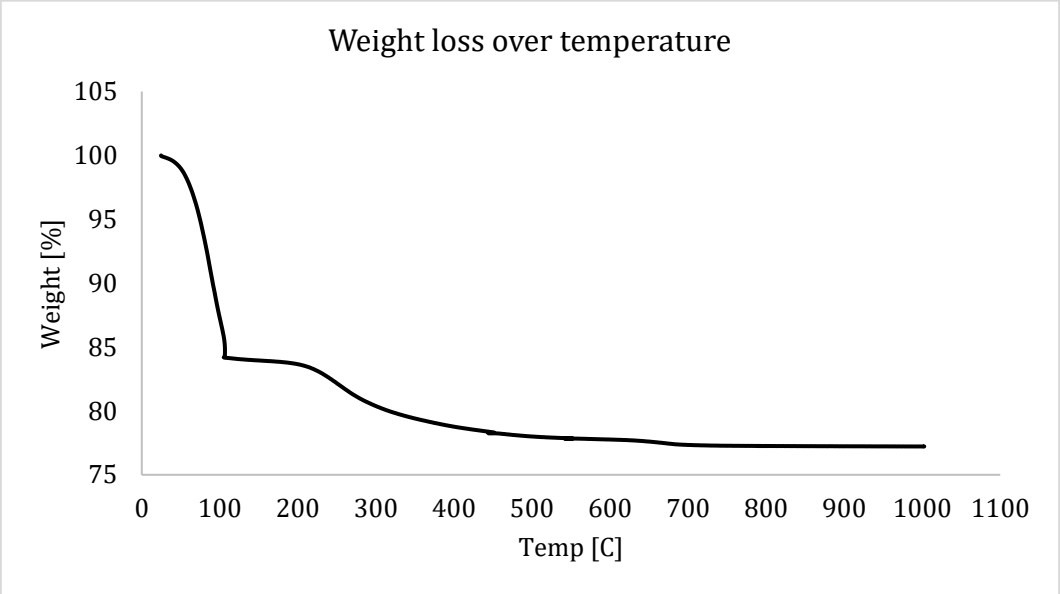

Figure 3-5: TGA -weight loss over temperature

The temperature at which the sample is completely dry and where all water is evaporated from the soil is at 105C. The figure above shows that from 23,6 to 105 C, 16% of weight is loss due to moisture. After 105°C, the gradient stops, and weight is then slowly lost from 105-1000°C. So, to calculate the OM, the weight loss over the interval 110-450 C is analyzed:

Table 3-2: Soil organic matter content

OM [g]	0,22517
Dry sample weight	3,21843
OM [%]	6,996268

3.3.2 Gradation test

Laser diffraction technique was used to identify the particle size distribution of the soil used in this experiment. The analysis was performed with a Malvern Mastersizer 2000, which measures the angular variation in intensity of light scattered from a laser beam that passes through a dispersed particulate sample from the studied soil. Large particles scatter light at small angles relative to the laser beam and small particles scatter light at large angles. Results are shown and analysed below.

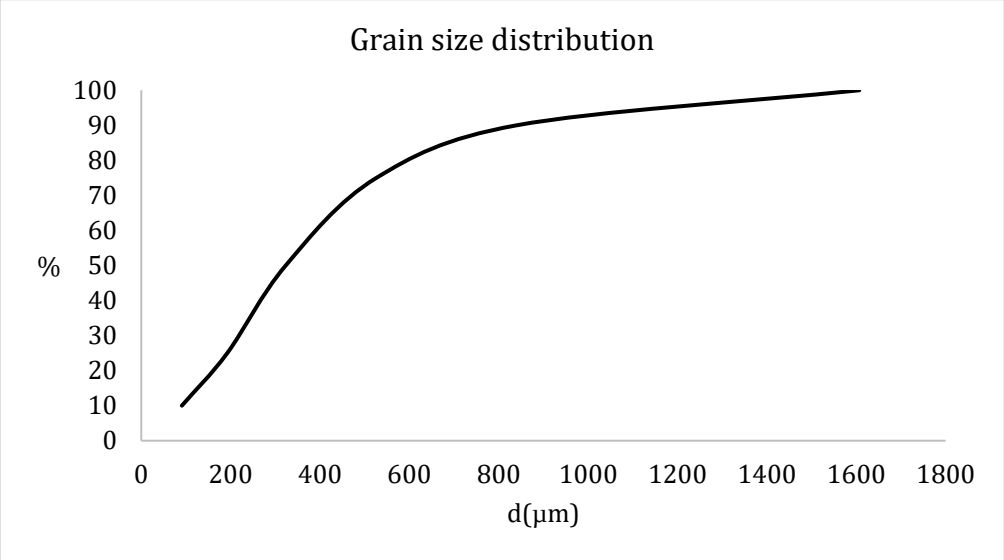

Figure 3-6: Particle size distribution

D [3, 2]: Surface area moment mean or Xsv

The mean surface area (Sauter Mean Diameter) in this soil sample was found to be equal to 0,163265.

This ratio is very relevant for this research, because the specific surface area has a direct influence in the bioavailability of the sample (Malvern Panalytical, n.d.). This value is most sensitive in fine particulates with low average size distribution.

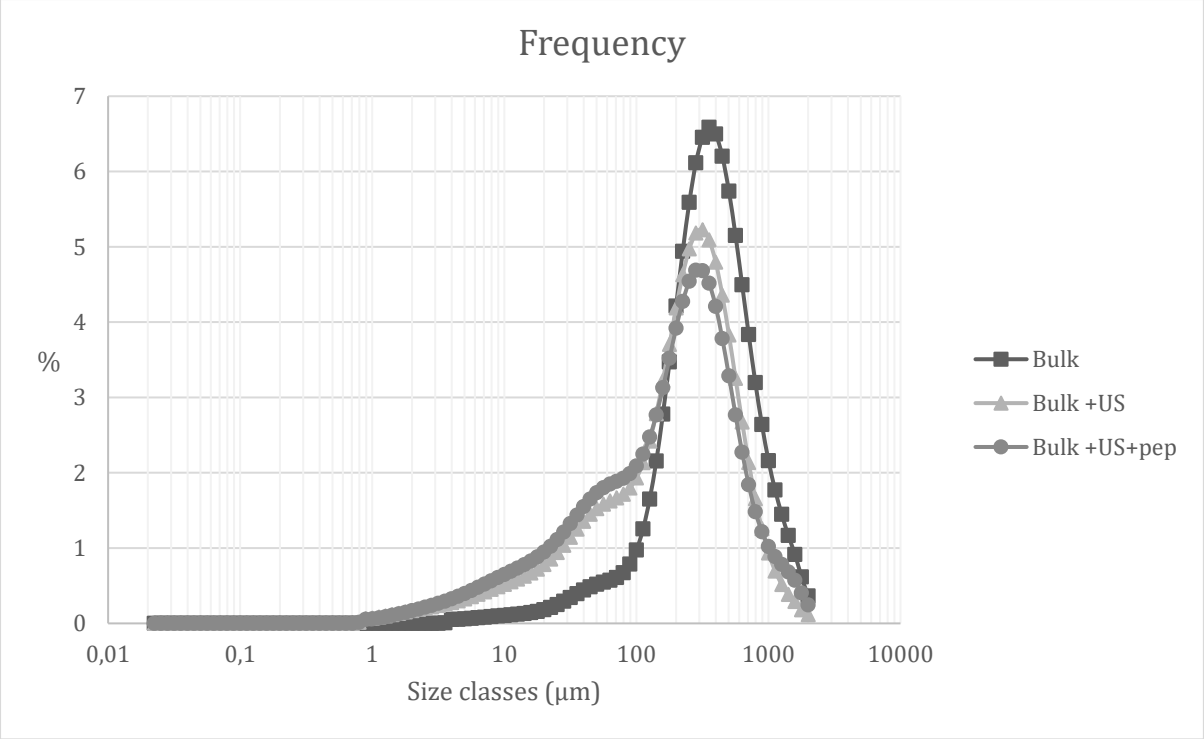

Figure 3-7: Composition analysis

3.3.3 Hydrus 2D

The experimental conditions that were used in this setup (Table 1) were also simulated in HYDRUS2D. The model was built using similar data to the one used in the tank experiment. For more detailed assumptions and results please refer to **Appendix A**, Input for the model can be found there too.

Boundary conditions, such as inlet or outlet flow were altered (constant head, constant flux or variable flux) to study the different water content scenarios and saturation values in the sandbox. The gap size of the fracture was also varied between 1 and 5cm width. These simulations were used to study their effect on the water saturation (θ) of the soil column as well as the solute transport phenomena.

Table 3-3: HYDRUS2D Parameters

Dimensions	Sandbox: 0,6m x 0,6m Bedrock: 0,1m thick x 0,250m width
Material Properties Distribution	**Loam**: Qr [-] = 0,078 Qs [-] = 0,43 α [1/m] = 3,6 n [-] = 1,56 Ks [m/day] = 0,2496 I [-] = 0,5 **Bedrock**:

	Qr [-] = 0,089 Qs [-] = 0,43 α [1/m] = 1 n [-] = 1,23 Ks [m/day] = 0 I [-] = 0,5
Initial Conditions	Pressure head has been left constant with a value of -1m for the whole soil column
Boundary Conditions	Top: Constant flux of 0.01m Sides: No flux Bottom: Free drainage
Particles	10 particles were allocated on top of the column, distributed uniformly
Output Information	10 days with 10 time-steps

The digital model used in these simulations, represents similar characteristics to the actual sandbox experiment that will be simulated in the laboratory. In this computer-based phase, a first approach to the relationship between theta (θ) and the bedrock gap size (fracture) was found, as well as the solute transport and water flow behaviour under different emulated field conditions.

Four observation points were studied, with following values for the latest day (30) of simulation:

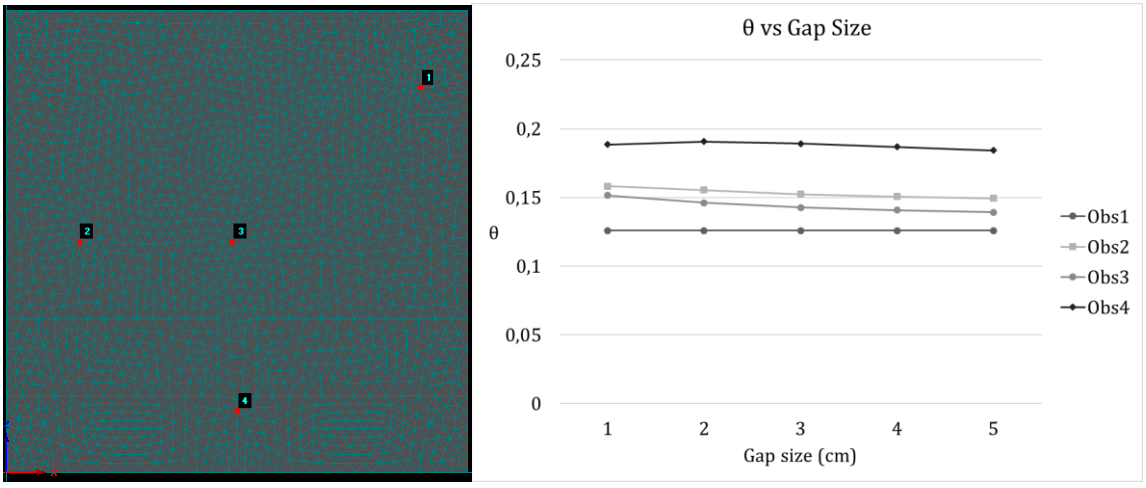

Figure 3-8: HYDRUS 2D simulation - Relationship between θ and gap size at day 30

From the results shown in Figure 3-8 it was found that, except for observation point 1, all other positions were influenced by the reduced gap size in their water content. Thus, from these simulations it can be

inferred that, the smaller the gap size in the fracture, the more water is retained by the soil on top of the fractured bedrock.

3.3.4 HYPROP

The hydraulic conductivity was calculated as a relationship between water content and the soil conductivity. As reviewed in section 3.3.4, the unsaturated hydraulic conductivity is given by the relationship between Ks and θ. This relationship was measured using HYPYOP technique, which combines the changes in mass and matric potential of a specific soil sample, collected from Griftpark. The measuring time was 6 days and Figure 3-9 shows the results of the unsaturated experiment, which relates the hydraulic conductivity as a function of saturation. The graph was plotted on a semi-logarithmic scale to visualize the exponential nature of the relationship.

The saturated hydraulic conductivity resulted in 0.407 [cm/d], which is the maximum value showed at saturation, which according to the graph corresponds to 33% of water content in the soil. It is also very clear how the hydraulic conductivity strongly decreases as the moisture content decreases from the saturation value.

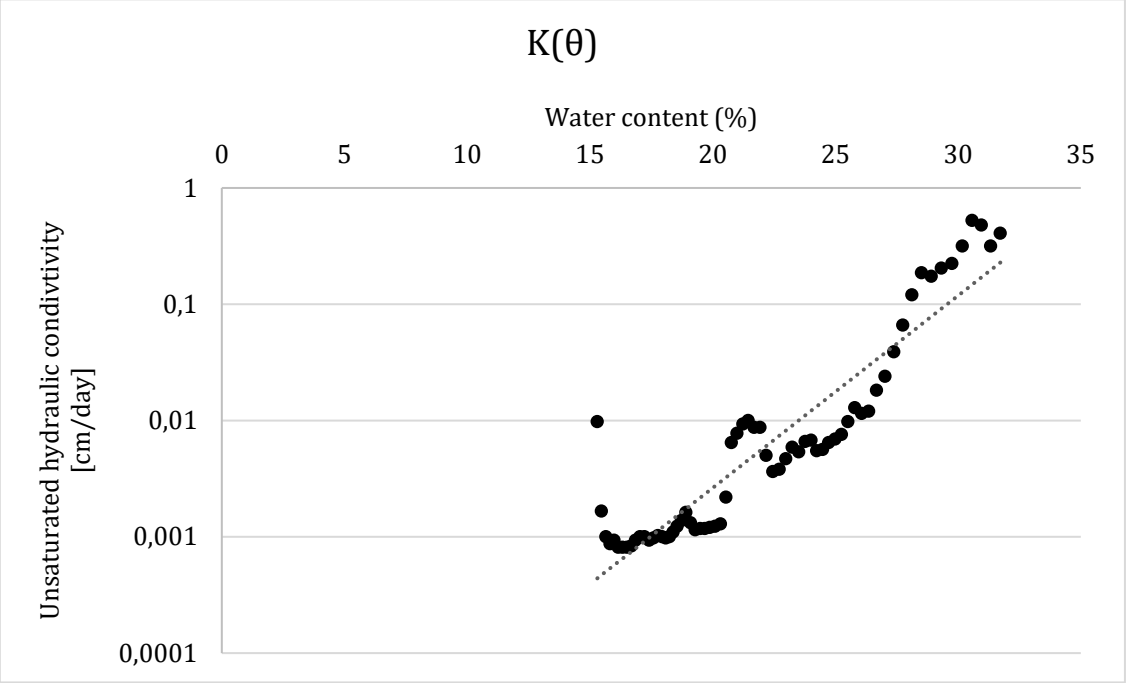

Figure 3-9: Hydraulic conductivity as a function of water content

4 Results

This chapter will introduce the results obtained in the laboratory work of this research. First, the nutrolase effect and the microbial activity in the soil will be put in perspective. Then, the tank preparation and injection procedure will be detailed and explained. Finally, the tank experiment will be outlined, explaining how the excess surface runoff as an artificial recharge process behaved within the sandbox, analysing the sensors readings.

4.1 Soil microbial activity

To test the effectiveness of the nutrolase to stimulate bacterial growth within the soil, twelve different soil samples were analysed with different concentrations of nutrolase (nutrients). Two types of soil were studied: natural soil saturated with rain and unsaturated sterile peat, testing smell, colour and structure in order to identify microbial activity in the samples.

For each soil sample a nutrolase dose was applicated. Different concentrations and dilutions of nutrolase were tested: 5ml of pure nutrolase; 3 ml of nutrolase with 3ml of water (1:1 dilution); 3 ml of nutrolase with 6ml of water (1:2 dilution); 3 ml of nutrolase with 9ml of water (1:3 dilution); 3 ml of nutrolase with 12ml of water (1:4 dilution).

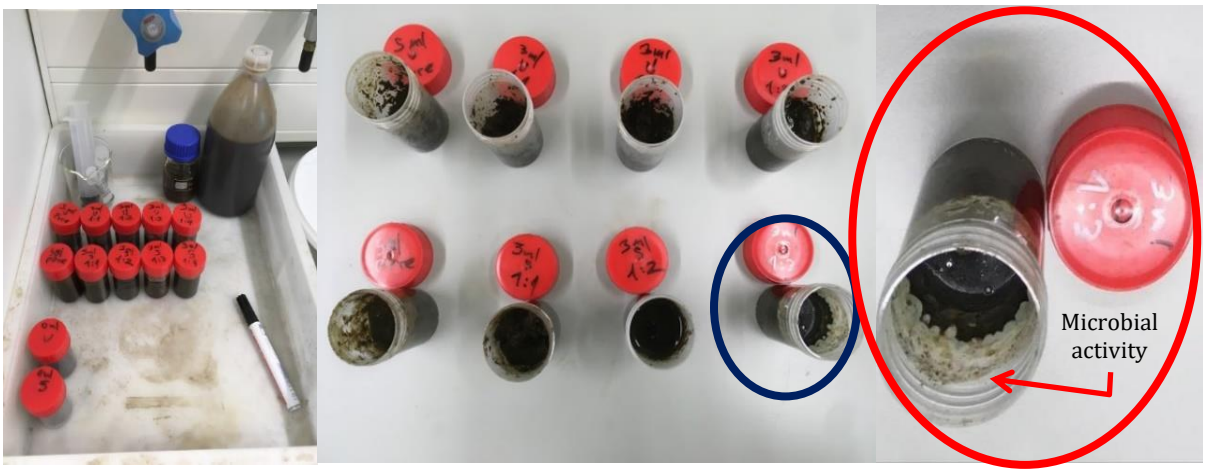

Figure 4-1: Soil samples with nutrolase application

Figure 4-1 depicts the different results after 1 week of nutrolase application. From the pictures it is very clear how the natural saturated soil sample was more affected by the 1:3 diluted nutrolase application (blue circle). Furthermore, when zooming in the 1:3 sample (red circle), the picture clearly shows physical signs of biomass growth in the vicinities of the soil sample (borders of the sample container).

Table 4-1 shows a summary of the nutrolase application, explaining the doses and effects that the different concentration of nutrolase had in the soil samples.

Table 4-1: Nutrolase effect in soil samples

Soil sample / Dilution	Natural Soil (smell/colour/structure)	Sterile peat (smell/colour/structure)
No nutrolase	No smell/brown/loose	No smell/brown/loose

1:1 (5ml water : 3ml nutrolase)	Smell/brown/tight	Smell/brown/tight
1:2 (3ml water : 3ml nutrolase)	Smell/dark brown/tight	Smell/dark brown/ tight
1:3 (3ml water : 6ml nutrolase)	Strong smell/dark brown/sturdy	Strong smell/dark brown/sturdy
1:4 (3ml water : 9ml nutrolase)	Strong smell/dark brown/ sturdy	Strong smell/dark brown/sturdy

4.2 Tank preparation

Before packing the column, all holes designated for insertion of the sensors were thoroughly closed with tapes, to prevent any loss of sand during packing procedure. The sand is also saturated with water, before, to facilitate the water flow, preventing thus fingering and preferential flows path.

The tank was then packed using the following procedure:

- Saturation of sand with water is done separately and before packing, layer by layer, to diminish the possibility of trapping air in enclosed pore spaces and preferential flows path formations.
- Step one was to fill the bottom part, by adding sand layers of 2cm height, which were then pressed on with a custom-made pestle, until field density is reached. The surface of the sand layers was then cautiously raked and scarified with sharp prongs to prevent horizontal layering.
- Step two was to carefully install the impermeable layer, avoiding any changes in sand conditions.
- Step three was to fill the top part, by adding the same 2cm layers and following the same procedure described in step 1. This way, the sand in the tank should now be as homogeneously as possible in terms of vertical porosity and hydraulic conductivity distribution.
- Finally, all sensors (tensiometers and 5TEs) are then horizontally inserted in to the column, by removing the tapes and carefully poking the sand from the outside, with a thin and sharp stick. Any gaps between the sensors and the holes crafted in the tank are sealed with silicon glue.

4.3 Injection

Water injection was done with a Masterflex L/S series Peristaltic Pump, keeping a constant 24/7 flux of 100 ml/h. The injection was divided into 2 inlets by means of two different tubes, to distribute the injection points evenly onto the topsoil. In order to create a constant and horizontal infiltration front, to avoid fingered and macropore flow, a mesh was also installed over the topsoil.

4.4 Tank experiment

A 2-day trial experiment was performed to test how the experimental setup behaves with the injection rates needed for the nutrolase application. Since the pump only functions in minutes, the total flux rate of 100ml/min was divided per 60 to transform the flowrate into ml/min. This gives a total of 1,7 ml/min, which was then divided into two different inlets at the top of the tank. The injection was performed via two different tubes at rates of 0,9 ml/min each, giving a final flux rate of 1,8 ml/min. With this flux rate, the

peristaltic pump was left overnight for 19 hours and 40 minutes, after which it was stopped to fix some technical problems encountered during the injection.

4.4.1 Initial conditions

Table 4-2 shows the initial conditions of the experiment, for each measured parameter, before the first water injection. The values were measured for 125 minutes and then averaged to get a single approximation.

The variance and standard deviation of the sample were also calculated to estimate the reliability of the data measured by the sensors in the tank.

Table 4-2: Initial conditions of the tank experiment

RECORD	Average	Variance	Std. Dev.
Ɛ 5TE(1)	5,85	0,00	0,020
Ɛ 5TE(2)	15,06	0,00	0,021
Ɛ 5TE(3)	7,03	0,00	0,040
Ɛ 5TE(4)	9,94	0,01	0,116
Θ 5TE(1)	0,10	0,00	0,000
Θ 5TE(2)	0,28	0,00	0,000
Θ 5TE(3)	0,13	0,00	0,001
Θ 5TE(4)	0,19	0,00	0,002
σb 5TE(1)	171,60	53,44	7,310
σb 5TE(2)	728,80	10,56	3,250
σb 5TE(3)	30,40	3,84	1,960
σb 5TE(4)	900,00	0,00	0,000
σp 5TE(1)	4.820,15	38.844,37	197,090
σp 5TE(2)	4.829,59	565,65	23,783
σp 5TE(3)	602,69	1.420,58	37,691
σp 5TE(4)	10.380,52	30.547,65	174,779
Tensio(1)	-25,95	2,11	1,453
Tensio(2)	-15,59	2,79	1,670
Tensio(3)	-5,94	1,65	1,284
Tensio(4)	-7,55	0,18	0,427

Table 4-2 shows stable values, except for some unexpected variations in the pore-water values, especially in sensors 1 and 4.

4.4.2 Matric Potential (Ψ)

Figure 4-2 shows the matric potential behaviour in the tank after approximately one day of injection and two days of measurements. The four red dots marked in the graph represent respectively the beginning of the experiment, the moment the pumping starts, the moment the pumping ends, and finally the end of the trial experiment.

The trial experiment started at 16-12-20 13:20. The datalogger and sensors recorded data every 5 minutes. After two hours, the pumping starts (15:25) and water starts dripping from the two inlets at a rate of 0,9 ml/min in each tube.

The water injection ends the next day (17-12-20) at 11:05, making a total injection of 19 hours and 40 minutes. Considering a flux rate of 0,9 ml/min per each tube, a total of 1,8ml/min is injected every minute

in the tank. The pump was left running a total of 19 hours and 40 minutes. Converting that value into minutes, results ins a total of 2124 minutes, meaning that 2.124 ml (2,124 litres) of water were injected into the tank.

Finally, the trial experiment ends after two days, finishing the 18-12-20 at 13:00.

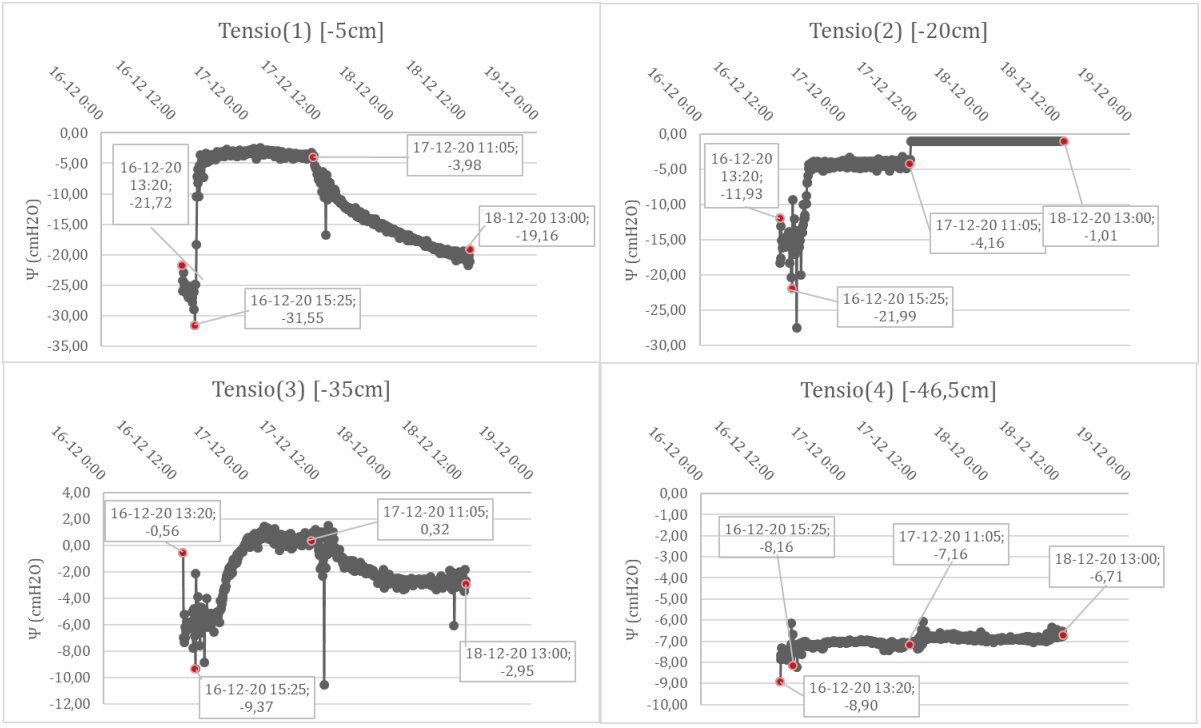

Figure 4-2: Tensiometers readings in 2 days trial

In Figure 4-2 Tensio 1 shows a decrease in water potential (less negative suction pressure) right after the water injection (pumping), reaching a constant value of -5 cmH_2O, during the pumping trial. After the pumping is finished, the pore suction begins to rise again, reaching almost its original value of -20 cmH_2O. This means that the water reached the 5 cm depth soon after the injection, and a constant infiltration front was formed in the middle vertical axis of the tank.

On the other hand, Tensio 2 shows a progressive decrease in water potential after the pumping starts. A constant value of -4 cmH_2O, is reached after approximately half a day (12 hours). Unexpectedly, after the pumping is finished, the pore suction increased, reaching a constant value of -1 cmH_2O, which is counterintuitive with respect to Tensio 1 values. The reasonable explanation then would be that the infiltration front reached a depth of 20 cm right after finishing pumping water into the tank.

Tensio 3 is one of the most indicatives sensors, as it is located just above the impermeable layer. It is very clear how the infiltration front causes a decreasing in water potential after the water injection. However, when comparing the curve with Tensio 2 graph, there is a longer distance and larger time travel, making a less steep slope, but reaching 0 cmH_2O approximately after 550 min (between 10:00 and 11:00) pm. Similar to what happened with Tensio 1, after the pumping is finished, the pore suction begins to rise again, but since water is still present in the vicinity of the impermeable layer, the pressure only drops to -2,95 cmH_2O.

The last and deepest (46,5cm) tensiometer, Tensio 4, shows almost no variations in its water potential. This can be explained by the fact that, during the two days of the experiment, a water table was formed on top of the impermeable layer. Thus, the water never reached the leakage and the matric potential stayed within a range of -9 to -7 cmH_2O, during the pumping trial. However, the pressure curve in the graph shows a slight positive slope in its shape.

4.4.3 Dielectric Permittivity (Ɛ)

Figure 4-3 shows the dielectric permittivity of the soil (Ɛ) and its behaviour in the tank, after approximately one day of injection and two days of measurements.

To determine the water content, bulk EC and pore-water EC the 5TE sensors use an oscillator running at 70 MHz to measure the dielectric permittivity constant of the surrounding soil (ε).

As reviewed in section 3.2.3, capacitance sensors, such as the 5TE measure the dielectric permittivity to estimate the water content, amongst other parameters such as the bulk electrical conductivity and the pore-water electrical conductivity.

Figure below shows the raw Ɛ values determined by the 4 different sensors installed in the side of the tank at depths z=-5, -20, -35, and -46,5 cm.

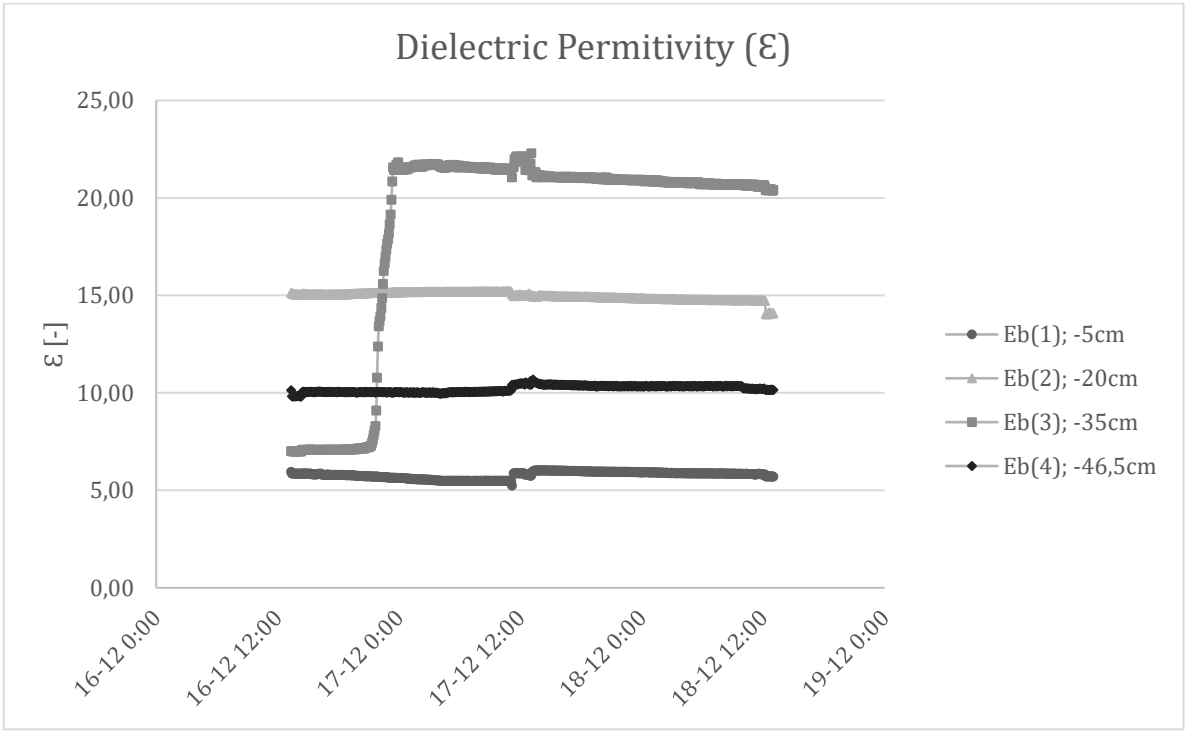

Figure 4-3: Dielectric permittivity values in 2 days trial

The graph clearly shows how the dielectric permittivity (Ɛ) is affected by the water injection at different depths in all 5TE sensors.

While in 5TE1 sensor, Ɛ stays constant during the whole experiment at 5, sensor 5TE2 Ɛ stays constant at 15. In sensor 5TE3, a clear fluctuation is shown after the pumping (15:25), spiking from 6 to 22, staying then more or less constant until the end of the experiment, with a decreasing tendency.

In sensor 5TE4, stays constant during the whole experiment at 10.

4.4.4 VWC (Θ)

Figure 4-4 shows the volumetric water content behaviour in the tank, after approximately one day of injection and two days of measurements. To determine the volumetric water content (θ), the 5TE sensors use the Topp equation (3.1), reviewed in section 3.2.3.1.

Volumetric water content is the volume of water per total volume of soil (V_W/V_T). For example, if a core soil sample with total volume of 100cm³ is composed by 15cm³, 35cm³ and 50cm³ of soil minerals, then the volumetric water content (θ) would be 35%. In some cases, VWC is also reported as cm³/cm³ or inches per foot.

Figure below shows the raw θ [cm³/cm³] values determined by the 4 different sensors installed in the side of the tank at depths z=-5, -20, -35, and -46,5 cm.

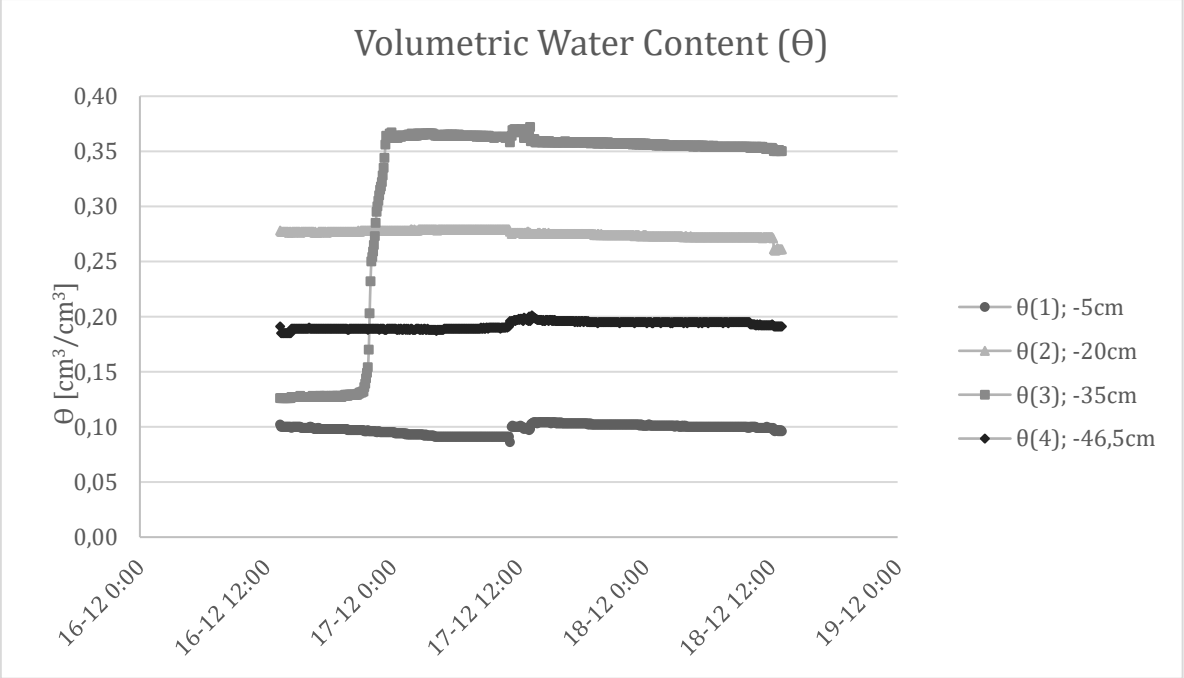

Figure 4-4: Volumetric water content in 2 days trial

From the figure above, it is noticeable how the volumetric water content (θ) is affected by water injection in all 5TE sensors differently.

While in sensor 5TE1, θ stays constant during the whole experiment at 5, sensor 5TE2 Ɛ stays constant at 15.

In sensor 5TE3, a clear fluctuation is shown after the pumping (15:25), spiking from 0,13 to 0,36, staying then more or less constant until the end of the experiment, with a decreasing tendency.

In sensor 5TE4, stays constant during the whole experiment at 10.

When comparing Figure 4-3 and Figure 4-4 it is clear how the volumetric water content is directly related to the dielectric permittivity (Ɛ) of the soil, being both curves almost equally shaped.

4.4.5 Bulk EC (σ_b)

Figure 4-5 shows the Bulk EC (σb) behaviour in the tank, after approximately one day of injection and two days of measurements. To determine the bulk EC, the 5TE sensors use the screws on the surface of the prongs to form a two-point electrical array in order to the measure EC of the soil (bulk).

The bulk soil EC is referred to the conductivity of the soil/water/air matrix and is a key parameter to measure dissolved solids and salts concentrations in the soil. Since the concentration of solids directly affects water conductivity, the EC is a very effective way of measuring salt concentrations in saturated and unsaturated soils. Furthermore, the bulk EC can be used to identify important benchmarks in the field. For instance, whenever the soil moisture (Θ) reaches a certain threshold (e.g. pF=2.5 or pF=4.2, field capacity or wilting point respectively), the bulk EC can be logged at that to compare it with other experimental values. This could be used to assess whether the nutrolase affects the bulk EC at certain Θ thresholds.

Figure below shows the raw bulk EC values determined by the 4 different sensors installed in the side of the tank at depths z=-5, -20, -35, and -46,5 cm.

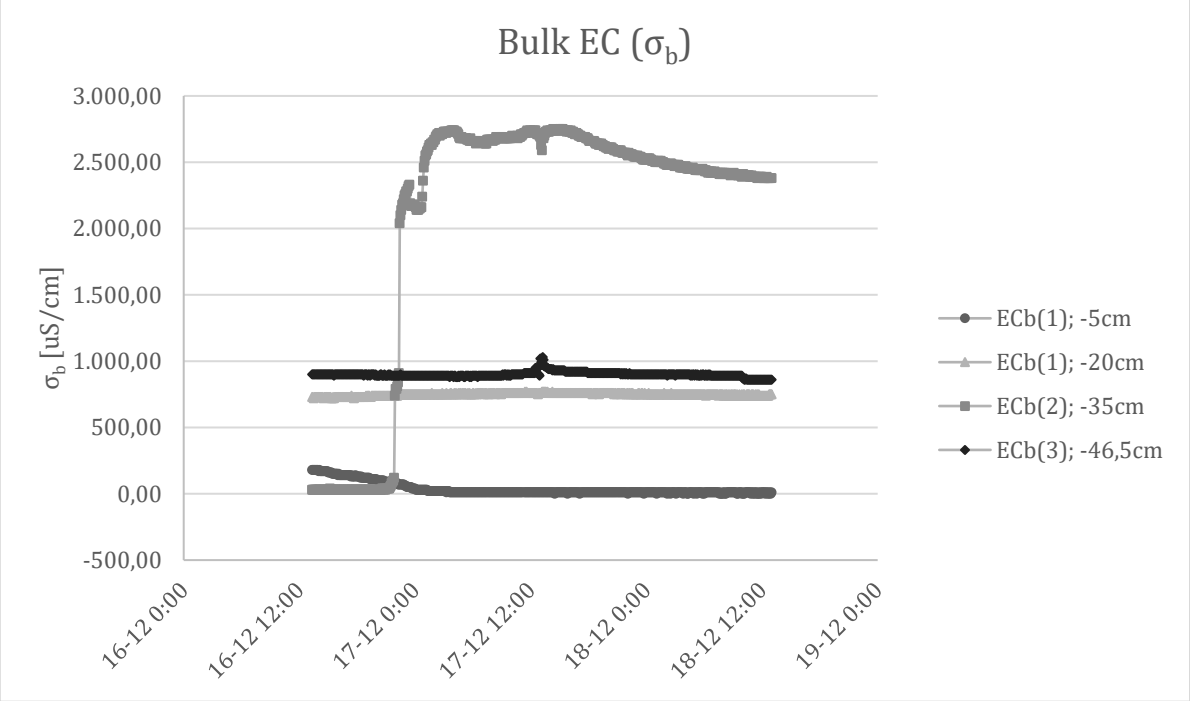

Figure 4-5: Bulk EC values in 2 days trial

From the figure above, it is clear how the bulk EC (σb) is affected by water injection in all 5TE sensors differently.

While in sensor 5TE1, σb stays constant almost during the whole experiment at approximately 750 uS/cm; sensor 5TE2, shows that the bulk EC starts at 250 uS/cm to decrease continuously until reaching the 0 value. Sensor 5TE3 depicts a clear EC increase after the pumping (15:25), spiking from 0 uS/cm to 2700 uS/cm with some fluctuations, and staying constant until the end of the experiment, with a decreasing tendency. Sensor 5TE4, shows that the bulk EC stays constant during the whole experiment at 900 uS/cm, because not enough water leaked through the gap for the sensor to read variations.

4.4.6 Pore-water EC (σ_p)

Figure 4-6 shows the Pore-water EC (σp) behaviour in the tank, after approximately one day of injection and two days of measurements. To determine the pore-water EC, the 5TE sensors use Hilhorst (1999) equation (3.2) reviewed in section 3.2.3.3. This equation offers the advantage to estimate pore-water EC values from bulk EC measurement in most type of soils.

Pore-water EC (σp), sometimes also referred to as soil water EC (σw) is defined as the electrical conductivity of the water present in the soil pores (Metergroup 2018). Similar to the bulk EC, the pore-water EC is used to measure dissolved solids and salts concentrations in the soil. However, the pore-water EC is the most effective parameter to measure solute concentrations in the soil, since the concentration of dissolved solids directly affects the conductivity of the water in the pores. Therefore, it should be more reliable than simply measuring bulk EC. Nonetheless, since the measured value stems from a mathematical approximation, results are subject to high uncertainties (please refer to section 3.2.3.3).

Figure below shows the raw pore-water EC values determined by the 4 different sensors installed in the side of the tank at depths z=-5, -20, -35, and -46,5 cm.

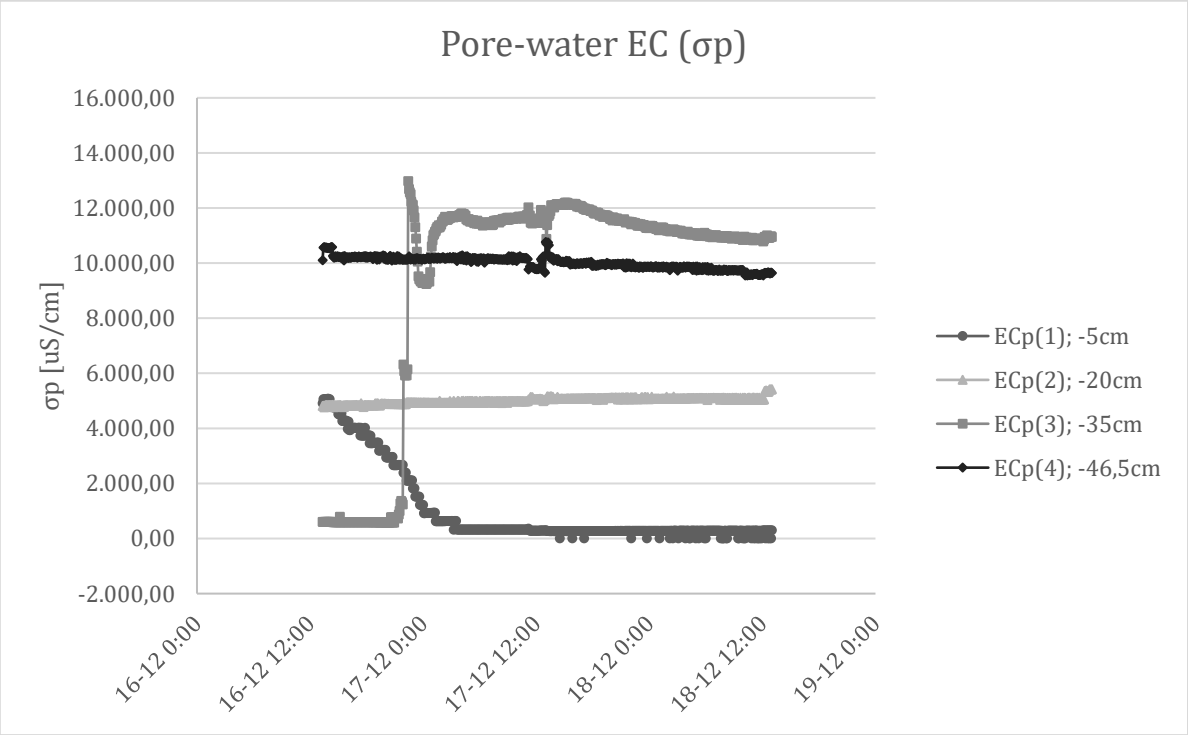

Figure 4-6: Pore-water EC values in 2 days trial

In this case, similar to Figure 4-5 sensor 5TE1, shows that pore-water EC starts at 5.000 uS/cm to decrease continuously until reaching 0. Sensor 5TE2 on the other hand, shows that pore-water EC stay constant almost during the whole experiment at approximately 5.000 uS/cm with an increasing tendency. Sensor 5TE3 shows a clear fluctuation after the pumping (15:25), spiking from almost 0 uS/cm to 13.000 uS/cm with some fluctuations, staying constant until the end of the experiment, with a slight decreasing tendency. Sensor 5TE4, stays constant at 10.000 uS/cm, because not enough water leaked through the gap for the sensor to read variations; however, it does show a decreasing tendency.

5 Discussion

This section will review the methodology applied in this experiment, analysing possible uncertainties, while also revisiting the accuracy and precision of the methods used in this study. The obtained results will be compared with theoretical approaches in order to assess their reliability and findings significance. Some recommendations for the second laboratory stage will be given as well, based on the experience gained in the 2-day trial (see section 4.4).

The water velocity can be calculated from Figure 4-2. Taking a look at Tensio(3), it is noticeable how the soil's suction pressure reaches 0 between 16-12-20 at 11:40 PM and 16-12-20 at 11:45 PM. Then the water velocity can be estimated with equation 5.1.

$$V = \frac{\Delta X}{T_{travel}} = \frac{35cm}{500min} \qquad 5.1$$

Using this approach, the water velocity is then equal to 0,07 [cm*min^{-1}] or 0,916 [m*day^{-1}]. However, as seen in section 3.3.4, the saturated hydraulic conductivity resulted in 0.407 [cm*day^{-1}] or equal to 0,00407 [m*day^{-1}] which is far from the actual velocity estimated with equation 5.1. Therefore, the estimation done in section 3.2.4, with HYPROP, should be revisited, using other approaches or fitting the experimental settings to field conditions, e.g. varying the bulk density of the core sample.

At this stage of the experiment, sensors 5TE1 and 5TE2 did not behave as expected, since in the 2-day pump trial they show only slight variations with respect to the dielectric permittivity, volumetric water content, bulk EC and the pore-water EC of the soil. It may also be that for sensors 1 and 2 air was trapped in the soil, affecting the final readings. Regarding sensor 5TE4, this should be analysed at a later stage of the experiment, since as seen in section 4.4.2, the injected water was not completely able to reach the fracture and only a little amount of liquid leaked through the 5cm gap.

As this study only focuses on the design and construction of an experimental setup, it should be considered as a first stage to prove the feasibility of the BioSealing technique in Artificial Recharge. Therefore, to prove that BioSealing is feasible in AR, a second stage of the experiment should be conducted, injecting nutrolase to the tank and monitoring how the parameters presented in this study vary with nutrient content in the soil. Attention should be paid to the volumetric water content especially at more shallow depths (z= {-5, -20}), due to the constant results obtained by the 5TE sensors in the first 2-day pumping trial. The gamma-ray transmission method is recommended to compare the porosity of the sand obtained with HYPROP and the volumetric water content (θ) obtained with the 5TE sensors.

To model the solute concentration within a constant soil saturation De Witte (2017) proposed a linear relationship between concentration of the input solution and the bulk EC. In his study, a calibration curve was made for each 5TE sensor, relating bulk EC and concentration (see equation 3.2 in section 3.2.3.3). Therefore, the concentration (C) of nutrolase in the soil can be found, either using the pore-water EC measured directly from the 5TE or calibrating the sensors with a certain moisture content and adding different concentrations of nutrolase to the soil, finding then a relationship between concentration [mol] and measured bulk EC.

Another recommendation would be not to cross contaminate water influent vessel, for which a second copy of the tubing pump is suggested. If this is not possible, then the tubing should be cleaned every time after nutrolase injection, to prevent clogging of inlets and outlets. The volume of nutrolase is replaced in the tank with three times water volume, therefore the complete pulse replacement is reached after 4 days (10L) of injection, meaning that the ideal injection of nutrolase is 3 times per week at even intervals (Monday, Wednesday, Friday). The nutrolase reservoir should be connected to the pump via a separated inlet and recipient.

As shown in section 4.1, the ideal dilution of nutrolase, is between 1:3 and 1:4, mixed with water first. This diluted solution should be used to fill the nutrolase reservoir, keeping a short injection time of 4 hours max to prevent the rotting of the nutrients and fluid. However, if the nutrient injection lasts for 4 hours, while keeping a 100ml/h flowrate, a 1:4 dilution makes 400 ml of 20% diluted nutrolase. Since only a limited amount of nutrolase is at disposal, a higher dilution (of 1:10 for instance) must be considered in the case that nutrolase runs out too quickly.

With respect to the recharge process, it is important to consider that a water table is recharged when excess water from rainfall or surface water infiltrates downward through the porous medium (soil) into the aquifer. It is important to highlight that the recharge area of an aquifer is given by the entire land overlying the water table. Therefore, when conducting a BioSealing experiment as an artificial groundwater recharge technique, the injection points should be evenly distributed onto or into the topsoil. For the purpose of this first trial experiment only two injection points were used, but it is recommended to have more injection points and the second phase of this experiment should also focus on how to better distribute the influents, both for water and nutrients.

According to the National Research Council (1994), Artificial Recharge (AR) is defined as the "…*process of spreading or impounding water on the land to increase the infiltration through the soil and percolation to the aquifer or of injecting water by wells directly into the aquifer"*. In accordance with this definition, any type of surface infiltration (e.g. rainwater harvesting, infiltration basins and canals, water traps, cutwaters) could be used to recharge unconfined aquifers. However, for confined aquifers, because of the presence of impermeable layers (without gaps), drainage wells are necessary in order to fully penetrate the aquifer and inject water into it. Thus, the BioSealing application in AR is recommended for unconfined aquifers, as it is much easier to implement.

Even though, in section 3.3.3 was found that the smaller the gap size in the fracture, the more water is retained by the soil on top of the fractured bedrock, some authors (Bouwer, 1982, Bouwer and Rice, 1984, National Research Council, 1994) argue that because of the particle settlement on the soil surface, a clogging effect is produced by the accumulation of suspended solids on the bottom and banks of the infiltration vicinities, hindering water infiltration through the top soil. Therefore, a thorough study should be made on the side effects that the clogging could have in the subsoil before scaling up this technology.

In this study, BioSealing is presented as an environmentally friendly technique that uses naturally present microorganism to seal the subsurface, in order to accumulate water on top of fractured bedrock. Normally, subsurface soil formations act as natural filters, removing different pollutants (physical turbidity, biological pathogens, and chemical compounds) as water percolates and travel through the soil. However, the water

quality of the infiltration system should be always monitored ideally before and after infiltration. Some techniques to monitor the water quality are reviewed in section 2.2.3, however these should be complemented with laboratory tests for a complete and thorough water quality analysis.

Moreover, AR techniques are not only used with natural water sources like stormwater runoff, but some methods may also include the use of treated sewage effluent as a recharge medium for groundwater. Nonetheless, if wastewater sources are to be used in AR, the optimal combination of treatment methods should be identified and applied before the injection process and after recovering the water from the aquifer. The use of treated wastewater as a recharge medium must also consider the health and environmental impacts of water reuse within the intervened ecosystem.

Some limitations during the experimental trial were noticed especially when measuring in-situ dielectric permittivity, volumetric water content, bulk EC and the pore-water EC of the soil. This could have been due to the sensors positioning, as they were installed on the side of the tank. The infiltration front could have been formed in the middle, leaving too much space between the prongs and the streamlines of the infiltration flow or void space could have affected the readings.

Furthermore, this experimental study was conducted in a specific region and environment with a certain type of soil, the data that was gathered could greatly differ from other soils in different areas or regions with different characteristics. Therefore, in order to validate the methodology constructed for this research, more experiments should be carried out, with different soil samples and approaches. A good follow-up would be to run the experiment with a different type of soil, found where the BioSealing application will be carried out and take a bottom-up approach, as it was done by Deltares in the first BioSealing trials.

Finally, as stated in the introduction, global economic development together with the climate change and the constant population growth is creating significant pressure on our global water resources. Therefore, artificial recharge techniques are expected to increase, in times where the sites available for dam construction become increasingly scarce and this technique could help providing an important solution for this complex societal challenge.

6 Conclusion

Even though groundwater has a natural recharge process which occurs when rainwater from rainfall and precipitation events spread on the surface land and topsoil, for the aquifer to be recharge, the water needs to travel long distances downwards in order to reach the water table depth, infiltrating into soils and percolating through pore spaces. This is a very complex physical chemical and biological process that cannot be replaced by artificial techniques, since it is part of the natural hydrological cycle.

Nonetheless, Artificial Recharge will be an important technique to be used in the near future, in order to improve the natural replenishment rate of groundwater resources, which are by far the most used by humankind. AR is normally used to recharge deep infiltration aquifers where the infiltration and percolation into subsurface is not effective enough to recharge these deep-water reservoirs. Thus, the main objective of AR applications is to store excess water in groundwater reservoirs for later use. Moreover, as discussed in the previous section, one important feature of AR is also related to water quality, since the subsurface soil formations normally act as natural filters, recharging aquifers with better water quality. Although AR is a common technique that has been largely implemented, the BioSealing application could serve as an important tool to artificially recharge unconfined and shallow aquifers. This could compliment the application of AR, that nowadays is mostly used in in deep infiltration aquifers, putting shallow and cheaper water resources aside. Hence, BioSealing is a relatively cheap and friendly engineering technique that has large potential to complement AR applications.

Additionally, BioSealing has proven to be a very useful soil repairing method in the views of both civil engineering and environmental geotechnics. So far, it has been used as a sustainable process to decrease the porosity of the soil, and mostly to repair leakages. It is presented as environmentally friendly technique as it is made of naturally present micro-organisms stimulated by natural occurring physical, chemical and biological processes by the addition of natural nutrients. Furthermore, the clogging effect has shown to be durable and effective solution because it stops the leakage after only weeks of application and does not reverse after stopping supply of nutrolase.

Further research should investigate other methods of injection, e.g. bottom-up, following the work done by Deltares. It is also important to explore other approaches to study the biomass growth in the soil and how to simulate the plugging of the gap. The relationship between time and hydraulic conductivity can be modelled in Hydrus, to simulate an approximate value for the clogging factor and the degree of soil plugging. The clogging process should also be further studied, since it remains unclear why and when the effect takes place. So far, the method has proven to be environmentally friendly and durable, although more research must be carried out to study the secondary effects and its actual durability within AR.

Finally, this research implemented a first laboratory environment to assess whether the application of the BioSealing technique is feasible in artificial groundwater recharge applications. Even though BioSealing is a common and useful technique for sealing leakages and preventing pollutants infiltration, it has not been yet applied to other engineering applications. This study should serve as a first stage experiment, to apply BioSealing as another useful geotechnical application to cope with current important societal issues, such as recurrent droughts and climate change.

7 References

Admiraal, B. J., & Molendijk, W. O. (2006). *Modification of soil-characteristics with biotechnology*. 18.

Barton, A. P., Fullen, M. A., Mitchell, D. J., Hocking, T. J., Liu, L., Wu Bo, Z., Zheng, Y., & Xia, Z. Y. (2004). Effects of soil conservation measures on erosion rates and crop productivity on subtropical Ultisols in Yunnan Province, China. *Agriculture, Ecosystems & Environment*, *104*(2), 343–357. https://doi.org/10.1016/j.agee.2004.01.034

Bezerra-Coelho, C. R., Zhuang, L., Barbosa, M. C., Soto, M. A., & van Genuchten, M. Th. (2018). Further tests of the HYPROP evaporation method for estimating the unsaturated soil hydraulic properties. *Journal of Hydrology and Hydromechanics*, *66*(2), 161–169. https://doi.org/10.1515/johh-2017-0046

Blauw, M., Lambert, J. W. M., & Latil, M. N. (2009). Biosealing: A Method for in situ Sealing of Leakages. *Ground Improvement Technologies and Case Histories*, 125–130. https://doi.org/10.3850/GI132

Bouwer, H. (1982). Design considerations for earth linings for seepage control. *Ground Water*, *20*(5), 531–5317.

Bouwer, H., & Rice, R. C. (1984). Hydraulic properties of stony vadose zones. Ground Water. *Ground Water*, *22*(6), 696–705.

Charbonneau, A., Novakowski, K., & Ross, N. (2006). The effect of a biofilm on solute diffusion in fractured porous media. *Journal of Contaminant Hydrology*, *85*(3–4), 212–228. https://doi.org/10.1016/j.jconhyd.2006.02.001

Council, N. R. (1994). *Ground Water Recharge Using Waters of Impaired Quality*. https://doi.org/10.17226/4780

de Marsily, G. (2007). An overview of the world's water resources problems in 2050. *Ecohydrology & Hydrobiology*, *7*(2), 147–155. https://doi.org/10.1016/S1642-3593(07)70180-5

de Witte, R. (2017). *Dispersivity-Saturation relationship for various porous media; Experiments and modelling*. 45.

Ellies, A.. (2000). Soil erosion and its control in Chile - An overview. Acta geológica hispánica, ISSN 0567-7505, Vol. 35, Nº 3-4, 2000 (Ejemplar dedicado a: Assesment of soil erosion and sedimentation through the use of the 137Cs and related techniques), pags. 279-284. 35.

EUREKA Conference and Working Session. (2016). *EUREKA 2016: 4th conference and working session: E!7614 APPL-EIS: schedule, proceedings: October 13th-14th, 2016, GEOtest, Inc., Brno University of Technology, Lednice, CZ* (Jana Pařílková & L. Procházka, Eds.). VUTIUM.

Fan, H., Hu, J., & He, D. (2013). Trends in precipitation over the low latitude highlands of Yunnan, China. *Journal of Geographical Sciences*, *23*(6), 1107–1122. https://doi.org/10.1007/s11442-013-1066-y

IPCC. (2019). *Summary for Policymakers—Special Report on Climate Change and Land*. https://www.ipcc.ch/srccl/chapter/summary-for-policymakers/

Lambert, J. W. M., Novakowski, K., Blauw, M., Latil, M. N., Knight, L., & Bayona, L. (2010). Pamper Bacteria, They Will Help Us: Application of Biochemical Mechanisms in Geo-Environmental Engineering. *GeoFlorida 2010*, 618–627. https://doi.org/10.1061/41095(365)59

Li, H., Tian, H., & Ma, K. (2019). Seepage Characteristics and Its Control Mechanism of Rock Mass in High-Steep Slopes. *Processes*, *7*(2), 71. https://doi.org/10.3390/pr7020071

Li, Y., Wang, Z., Zhang, Y., Li, X., & Huang, W. (2019). Drought variability at various timescales over Yunnan Province, China: 1961–2015. *Theoretical and Applied Climatology*, *138*(1–2), 743–757. https://doi.org/10.1007/s00704-019-02859-z

Liao, H., Zhao, K., Lambert, J. W. M., & Veenbergen, V. (2007). *EXPERIMENTAL STUDY ON BIOSEALING TECHNOLOGY FOR SEEPAGE PREVENTION*. 8.

Lü, J., Ju, J., Ren, J., & Gan, W. (2012). The influence of the Madden-Julian Oscillation activity anomalies on Yunnan's extreme drought of 2009–2010. *Science China Earth Sciences*, *55*(1), 98–112. https://doi.org/10.1007/s11430-011-4348-1

Malvern Panalytical. (n.d.). *Particle Characterization—Guide to Particle Characterization Methods*. https://www.malvernpanalytical.com/en/learn/knowledge-center/Whitepapers/WP120620BasicGuidePartChar

Marlet, G. (1999, September 17). *Buurtbewoners omarmen hun oude gifpark*. Trouw. https://www.trouw.nl/gs-b9dc6e64

Metergroup. (2018). *5TE Manual*. Metergroup. http://publications.metergroup.com/Manuals/20435_5TE_Manual_Web.pdf

OECD. (2016). *Mitigating Droughts and Floods in Agriculture: Policy Lessons and Approaches*. OECD. https://doi.org/10.1787/9789264246744-en

Pařílková, J, Gjunsburgs, B., Zachoval, Z., Veselý, J., & Műnsterová, Z. (2017). Earth-Fill Dam Monitored by EIS Method during Application of Nutrient Aqueous Solution used in BioSealing Method. *IOP Conference Series: Materials Science and Engineering*, *251*, 012130. https://doi.org/10.1088/1757-899X/251/1/012130

Ross, N. (2004, June 1). *Biobarriers & Fractured Rock*. Canadian Consulting Engineer. https://www.canadianconsultingengineer.com/features/biobarriers-fractured-rock/

Ross, N., & Bickerton, G. (2002). Application of Biobarriers for Groundwater Containment at Fractured Bedrock Sites. *Remediation Journal*, *12*(3), 5–21. https://doi.org/10.1002/rem.10031

Ross, N., Novakowski, K. S., Lesage, S., Deschênes, L., & Samson, R. (2007). Development and resistance of a biofilm in a planar fracture during biostimulation, starvation, and varying flow conditions. *Journal of Environmental Engineering and Science*, *6*(4), 377–388. https://doi.org/10.1139/s06-056

Ross, N., Villemur, R., Deschênes, L., & Samson, R. (2001). Clogging of a limestone fracture by stimulating groundwater microbes. *Water Research*, *35*(8), 2029–2037. https://doi.org/10.1016/S0043-1354(00)00476-0

Tarhule, A. (2017). The Future of Water. In *Competition for Water Resources* (pp. 442–454). Elsevier. https://doi.org/10.1016/B978-0-12-803237-4.00025-2

van Beek, V. M. (2007). *BIOSEALING, A NATURAL SEALING MECHANISM THAT LOCATES AND REPAIRS LEAKS*. 8.

van Paassen, L. A. (2011). Bio-Mediated Ground Improvement: From Laboratory Experiment to Pilot Applications. *Geo-Frontiers 2011*, 4099–4108. https://doi.org/10.1061/41165(397)419

Weersma, S., van Tol, A., van der Hoek, E., Veenbergen, V., & Lambert, J. (2005). BioSealing: How micro-organisms become our little allies in repairing leaks in underground constructions. In Y. Erdem & T. Solak (Eds.), *Underground Space Use. Analysis of the Past and Lessons for the Future*. Taylor & Francis. https://doi.org/10.1201/NOE0415374521.ch87

Whitmore, T. J., Brenner, M., Engstrom, D. R., & Xueliang, S. (1994). Accelerated soil erosion in watersheds of Yunnan Province, China. *Journal of Soil and Water Conservation*, *49*(1), 5.

W.O, M., W.H, van der Z., & G.A.M, van M. (2009). SmartSoils, Adaptation of soil properties on demand. *Stand Alone*, 2443–2446. https://doi.org/10.3233/978-1-60750-031-5-2443

Ws and Wg—Technical report on water scarcity and drought man.pdf. (n.d.). Retrieved January 10, 2021, from

Ws, M., & Wg, D. (2007). Technical report on water scarcity and drought management in the Mediterranean and the Water Framework Directive. *Mediterranean Water Scarcity and Drought Report*, 142. Retrieved from http://www.emwis.net/topics/WaterScarcity/PDF/MedWSD_FINAL_Edition

Ziolkowski, B., & Ziolkowska, J. R. (2017). Product, Process, and Organizational Innovations in Water Management. In *Competition for Water Resources* (pp. 403–422). Elsevier. https://doi.org/10.1016/B978-0-12-803237-4.00023-9

Appendices

A. Hydrus 2D

In these simulations, different injection rates and injection durations were tested. The first suggestion made by Deltares (Bas van der Zaar) was an injection rate of 100ml/h. To convert that value to m3/h, the flow rate was divided that by the circular area of the pipe, which is between 6mm and 5mm. Using these diameters, the model yields a 1D injection rate of 0.035 m/h and 0.05 m/h respectively. This shows that the smaller the diameter, the faster the injection rate.

Regarding the injection duration, in Deltare's experiment the injection was done with 15ml shots of 4 times diluted nutrolase once a day, 5 times a week, for an hour at 100ml/h. By using these input values in the simulation, the nutrolase reaches the gap at 2.92 or 2.04 days depending on the injection rate (Table A-1). This may seem relatively slow, so it is necessary to increase the duration of injection, maintaining a 1:4 dilution. So, for example, if the duration is increased by 2 hours instead of 1, then 200ml of water will be injected to the soil column and another 15ml shot of nutrolase should be added to maintain the ratio. The same applies for a 5-hour duration with 5 shots of diluted nutrolase. As Table A-1 shows, increasing the duration of the injection helps reducing the travel time to the gap. In addition, adding more shots of diluted nutrolase, as a consequence of increasing the duration, means that there will be more nutrolase concentration at the gap.

An estimation of how much pure nutrolase is used for each experiment was performed and it was concluded that 15ml shots of 4 times diluted nutrolase would mean, 3.75ml of pure nutrolase. Assuming a 5-hour injection, each day, would give a total of 93.75ml per week for the experiment., which is accordingly to the nutrolase amount at disposal.

So, for instance, assuming a 6 weeks for the biofilm formation —common value found in the literature review—, then the total amount of pure nutrolase to be used is 93.75ml x 6 weeks x 10 = 5625ml = 5.625 L, and 20L of pure nutrolase are at disposal.

0.03m radius = 0.035 (m/h)

0.025m radius = 0.05 (m/h)

Table A-1: Simulation of nutrolase injection with HYDRUS2D

TRAVEL TIME TO 1 GAP (Days)		**Injection Rate (m/h)**		**Total pure nutrolase used after 1 week of injection (ml)**
		0.035	0.05	
Injection Duration (hours per day for 5 days)	1	2.92	2.04	18.75ml
	2	1.54	1.125	37.5ml

	5	0.45	0.29	93.75ml

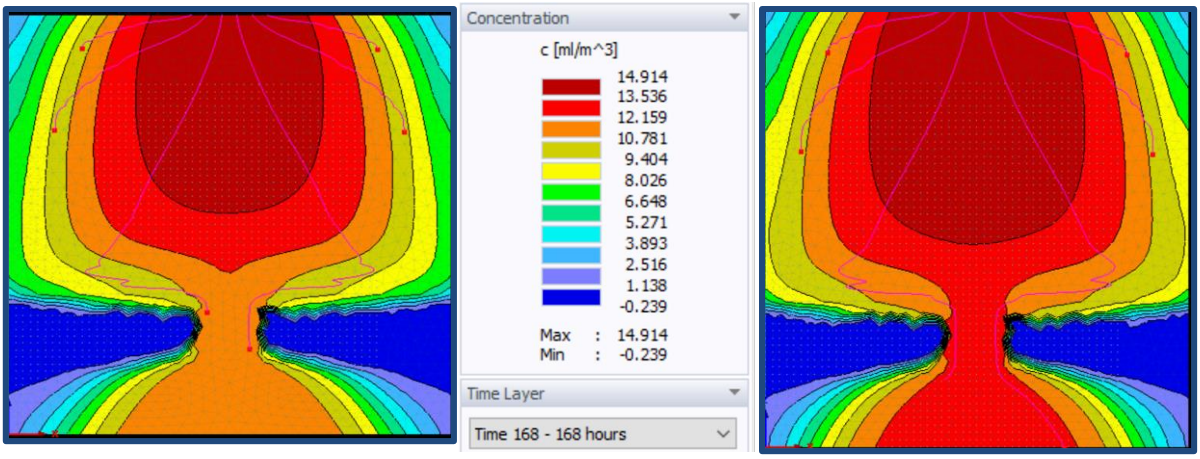

Figure A-1 HYDRUS 2D simulation - Nutrolase concentration

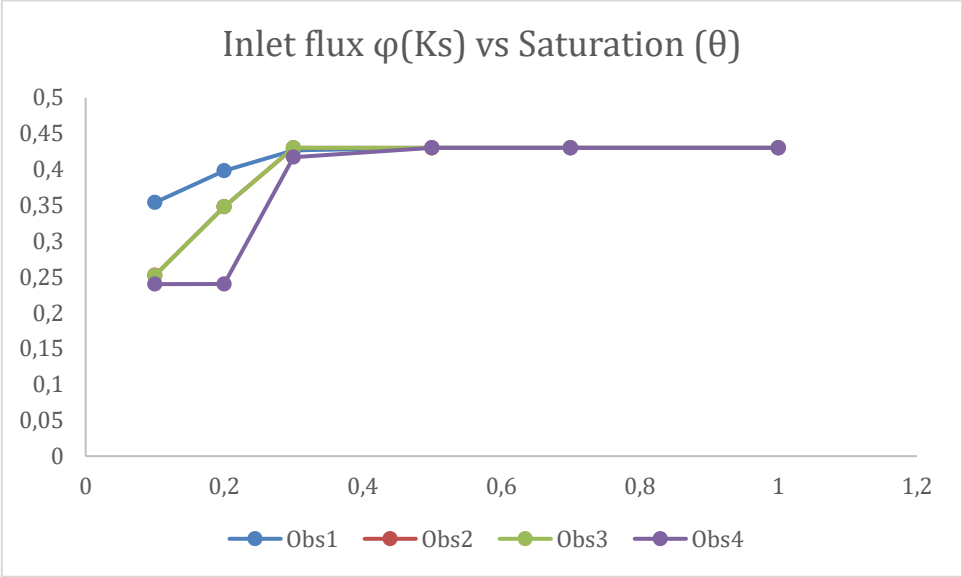

Figure A-2: Inlet flux φ(Ks) vs Saturation (θ)

After 24 hours of simulation, using the inlet flux as a function of the saturated hydraulic conductivity (Ks), the following behaviour was found:

- If the Inlet flux > 1,22*Ks (0,0126809m/h) → The Hydrus2D model collapses and does not converge.
- If the Inlet flux 0,5*Ks < inlet flux < 1,22*Ks → The Hydrus2D model reaches full saturation (Qs).
- If the Inlet flux < 0,5*Ks → The Hydrus2D model does not reach full saturation (Qs).

B. *Experimental setup*

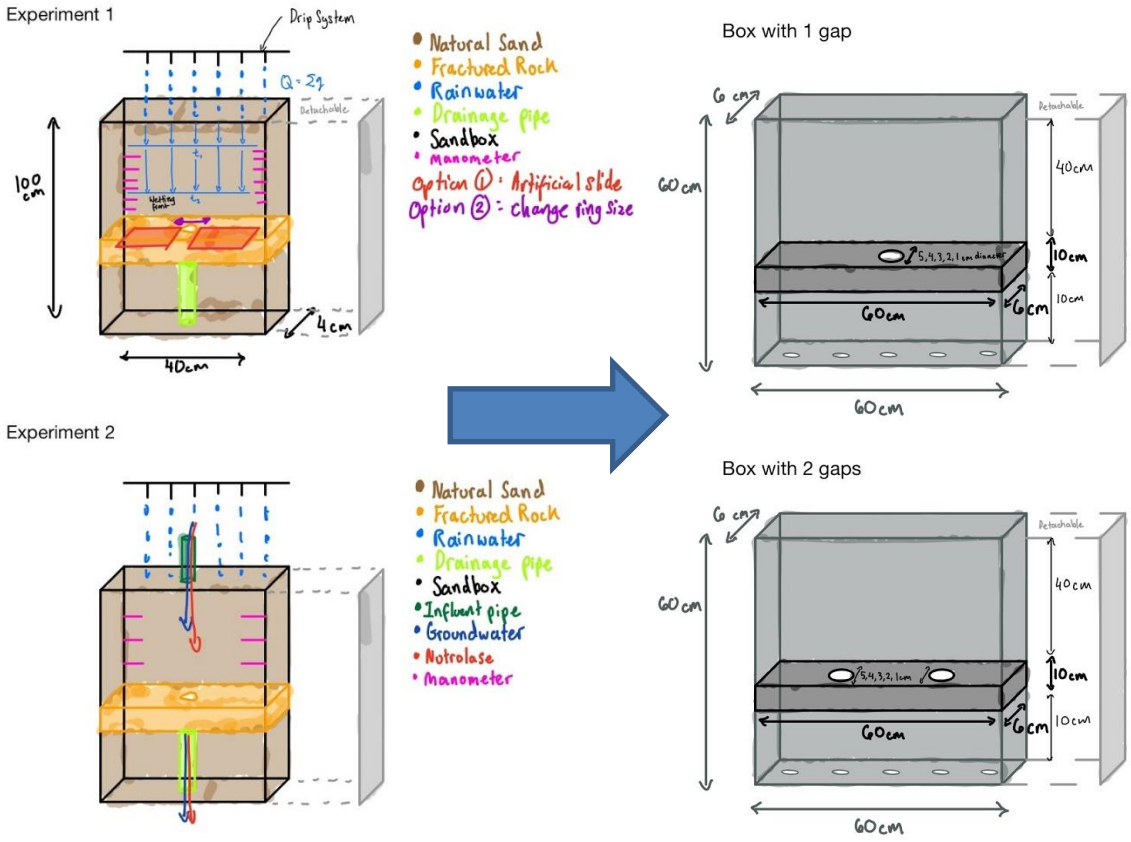

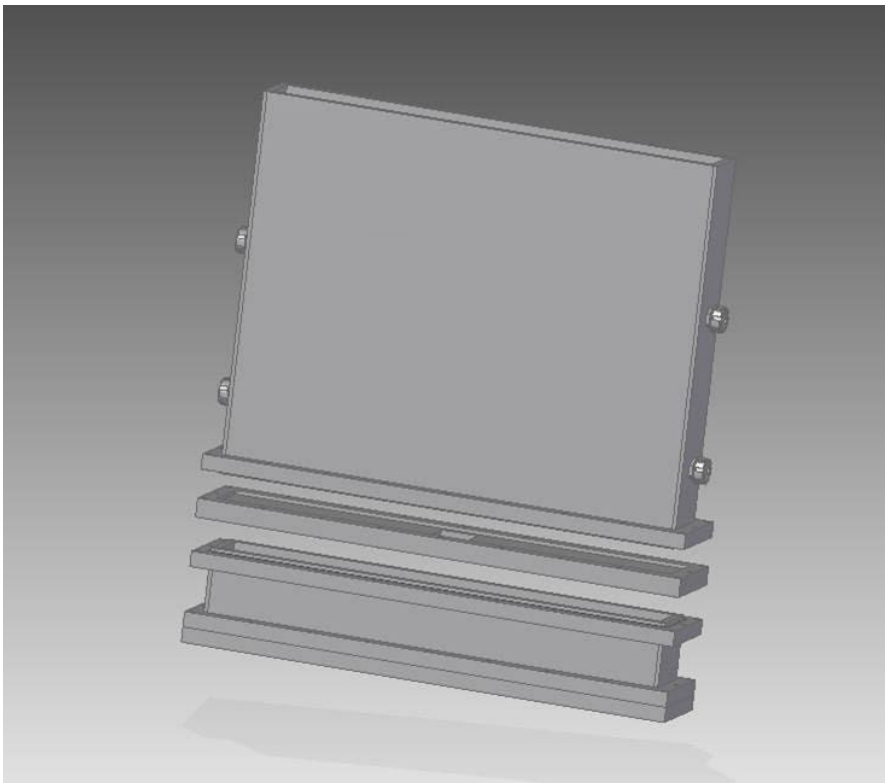

Figure B-1: Conceptual designs

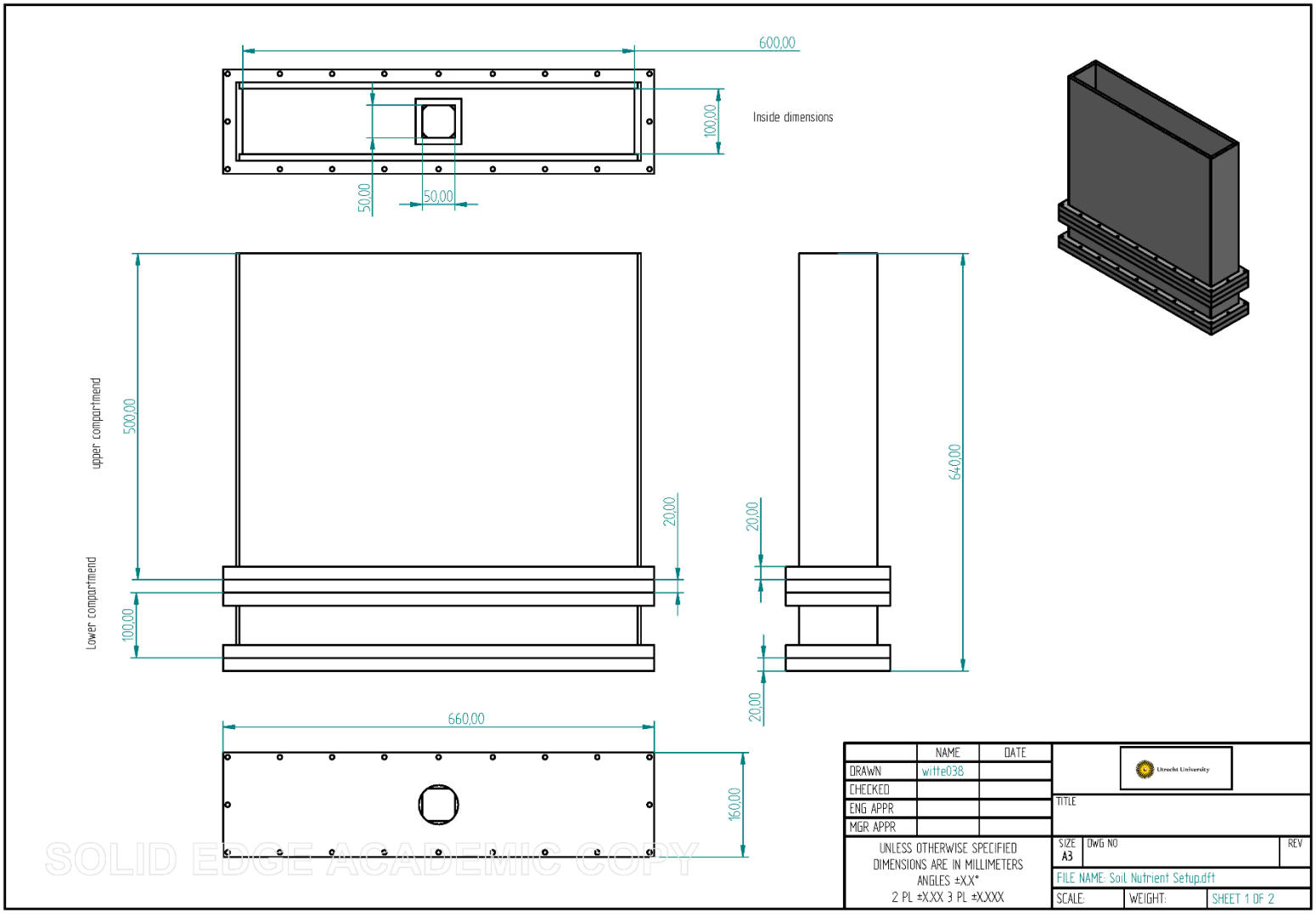

Figure B-2 BioSealing setup detailed design - outside

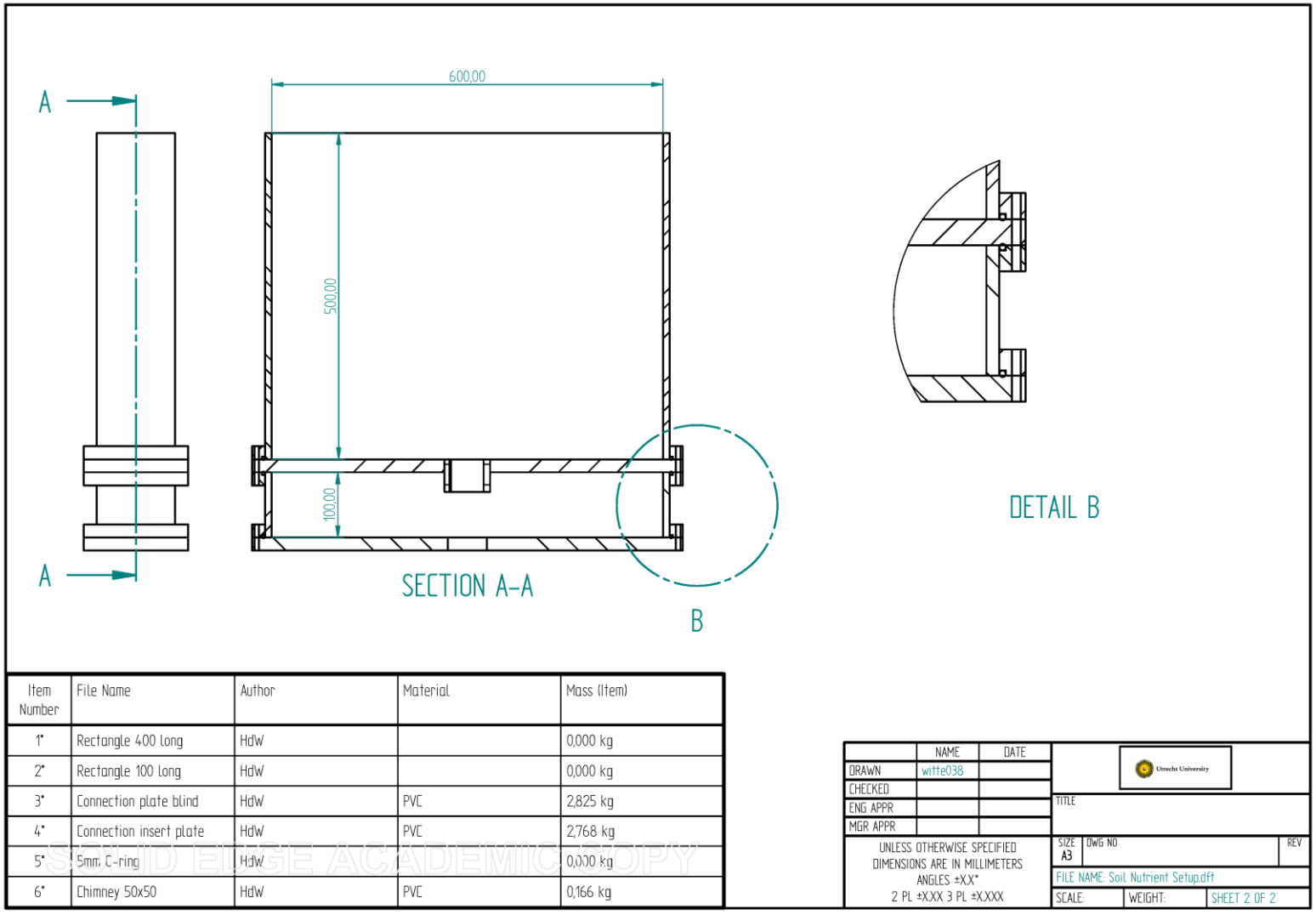

Item Number	File Name	Author	Material	Mass (Item)
1"	Rectangle 400 long	HdW		0,000 kg
2"	Rectangle 100 long	HdW		0,000 kg
3"	Connection plate blind	HdW	PVC	2,825 kg
4"	Connection insert plate	HdW	PVC	2,768 kg
5"	5mm; C-ring	HdW		0,000 kg
6"	Chimney 50x50	HdW	PVC	0,166 kg

	NAME	DATE
DRAWN	witte038	
CHECKED		
ENG APPR		
MGR APPR		

UNLESS OTHERWISE SPECIFIED
DIMENSIONS ARE IN MILLIMETERS
ANGLES ±X.X°
2 PL ±X.XX 3 PL ±X.XXX

Utrecht University

TITLE

SIZE A3 | DWG NO | REV

FILE NAME: Soil Nutrient Setup.dft

SCALE: | WEIGHT: | SHEET 2 OF 2

Figure B-3 BioSealing setup detailed design – cross section

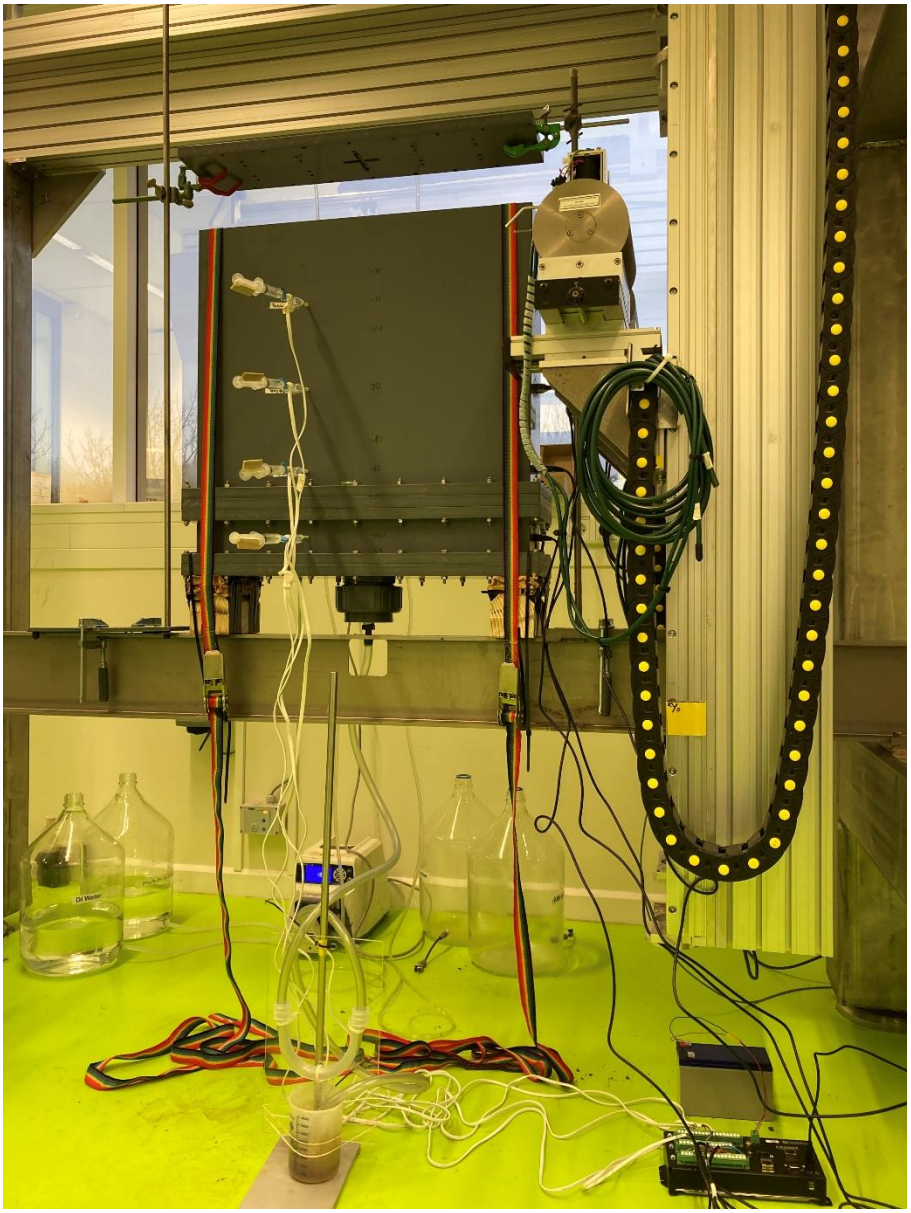

Figure B-4 BioSealing setup final design

C. Soil sampling

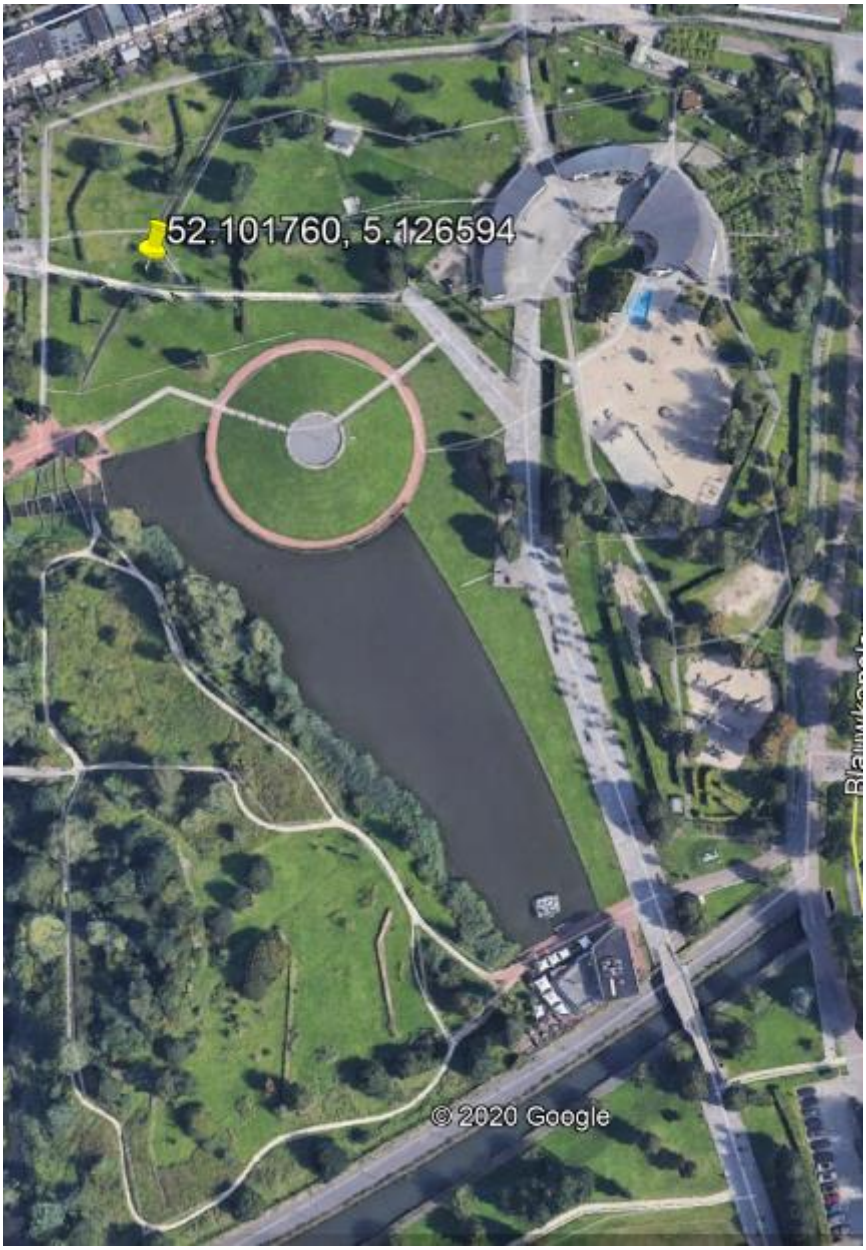

Figure C-1: Sample coordinates (Griftpark, google earth 2020)

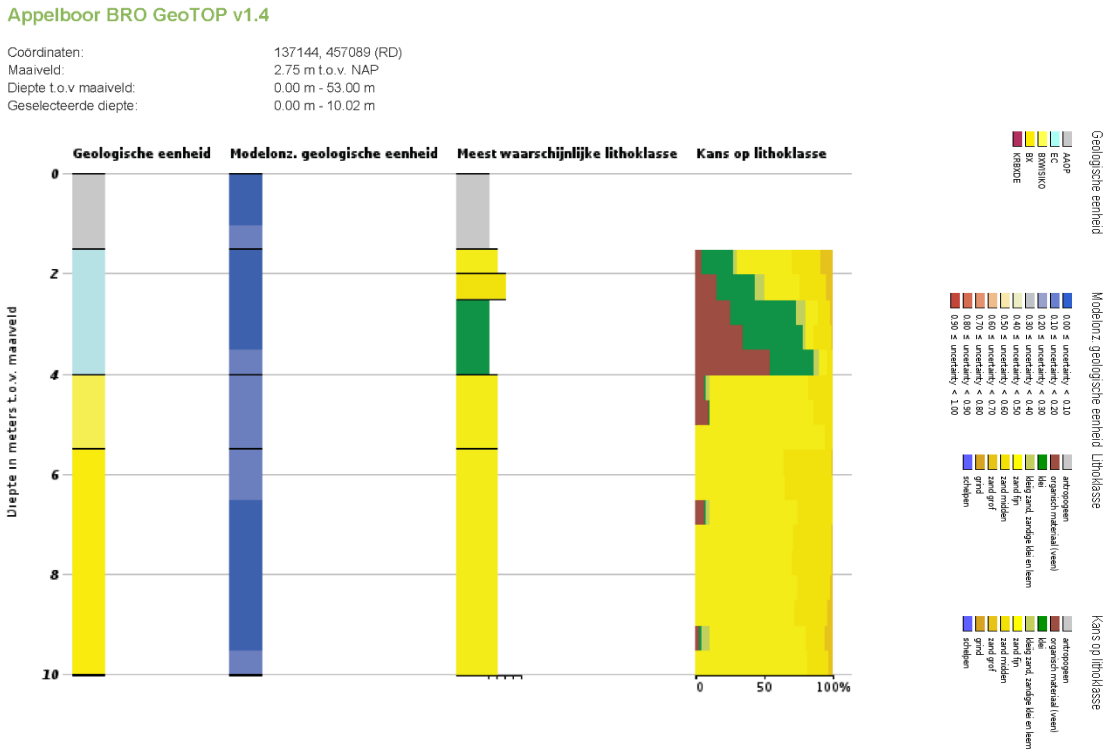

Figure C-2: Type of soil (profile at coordinates 10m deep, TNO)

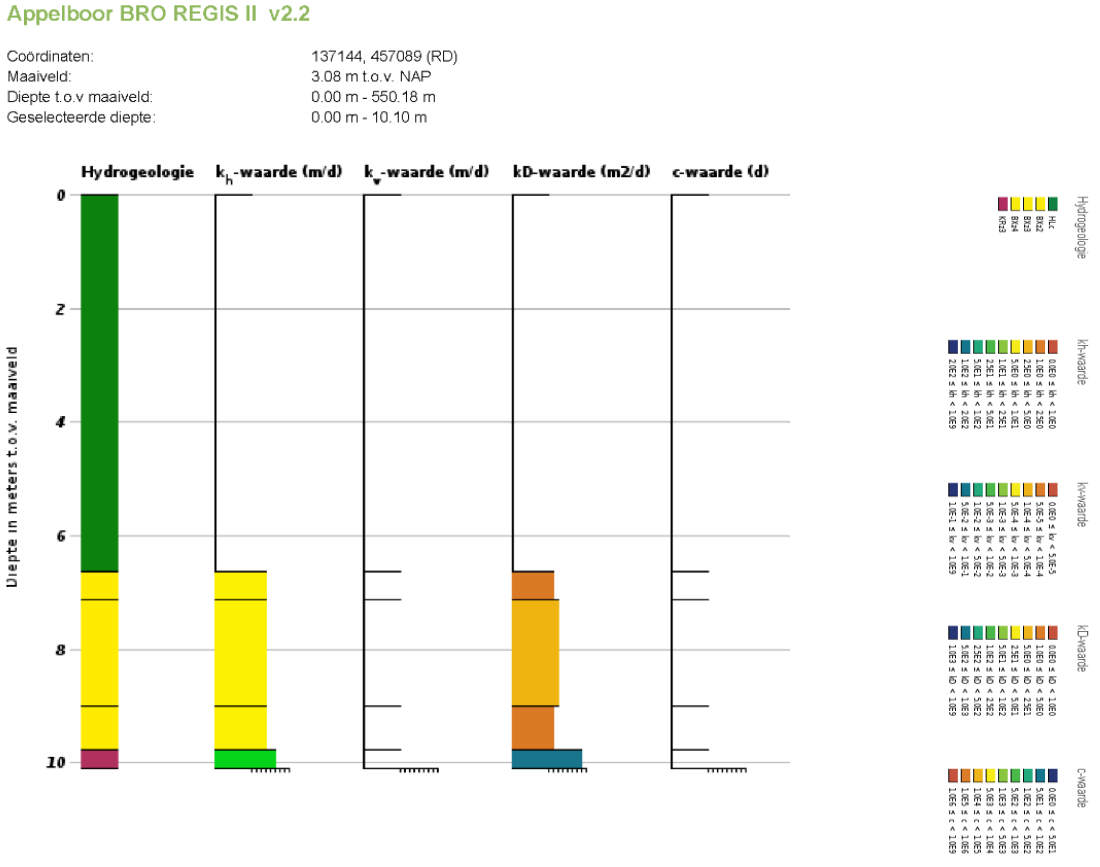

Figure C-3: Soil properties (profile at coordinates 10m deep, TNO)

D. Calibration Data

5TE Sensors EC vs θ

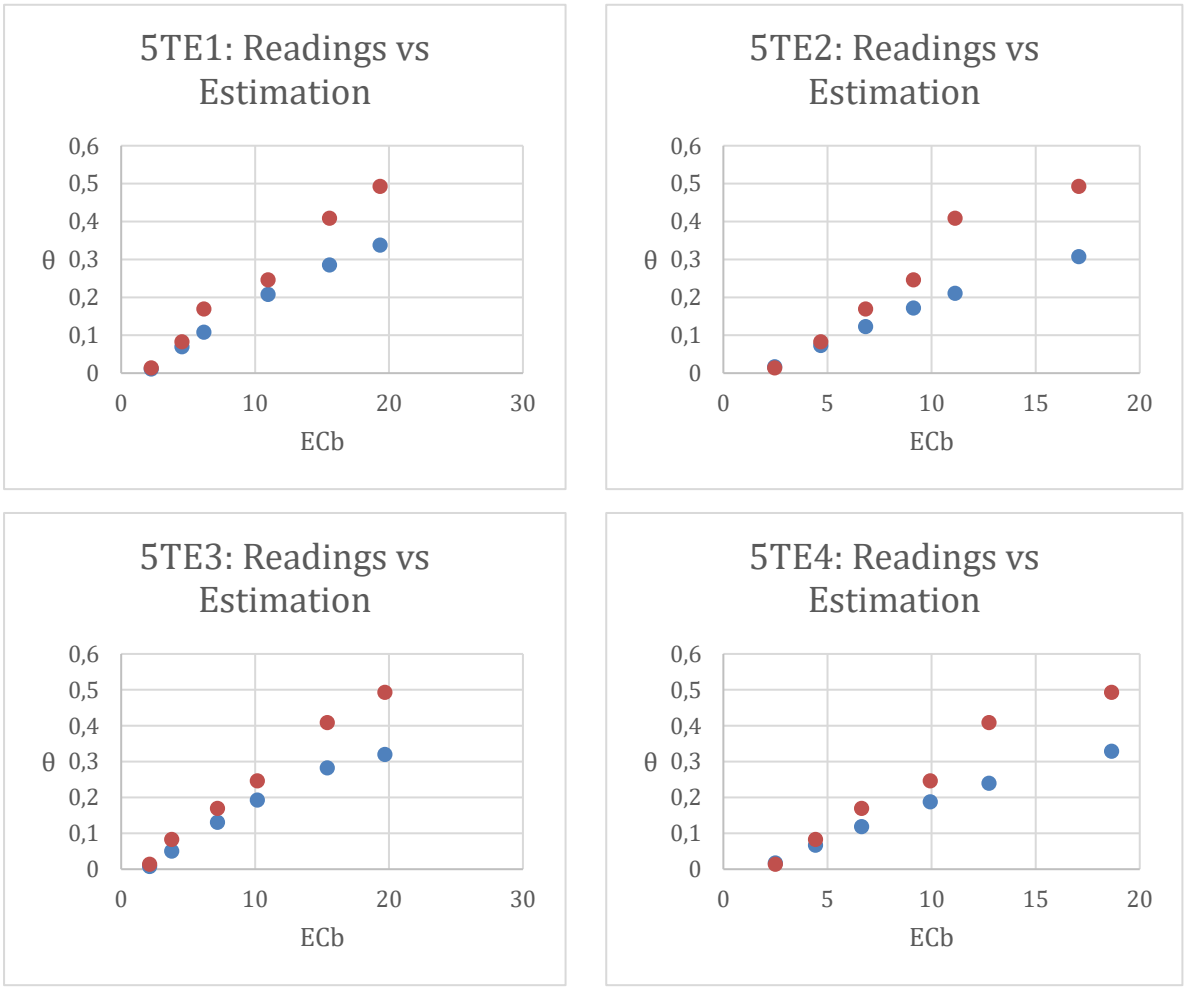

Figure D-1: 5TEs calibrationcurve vs raw data curve

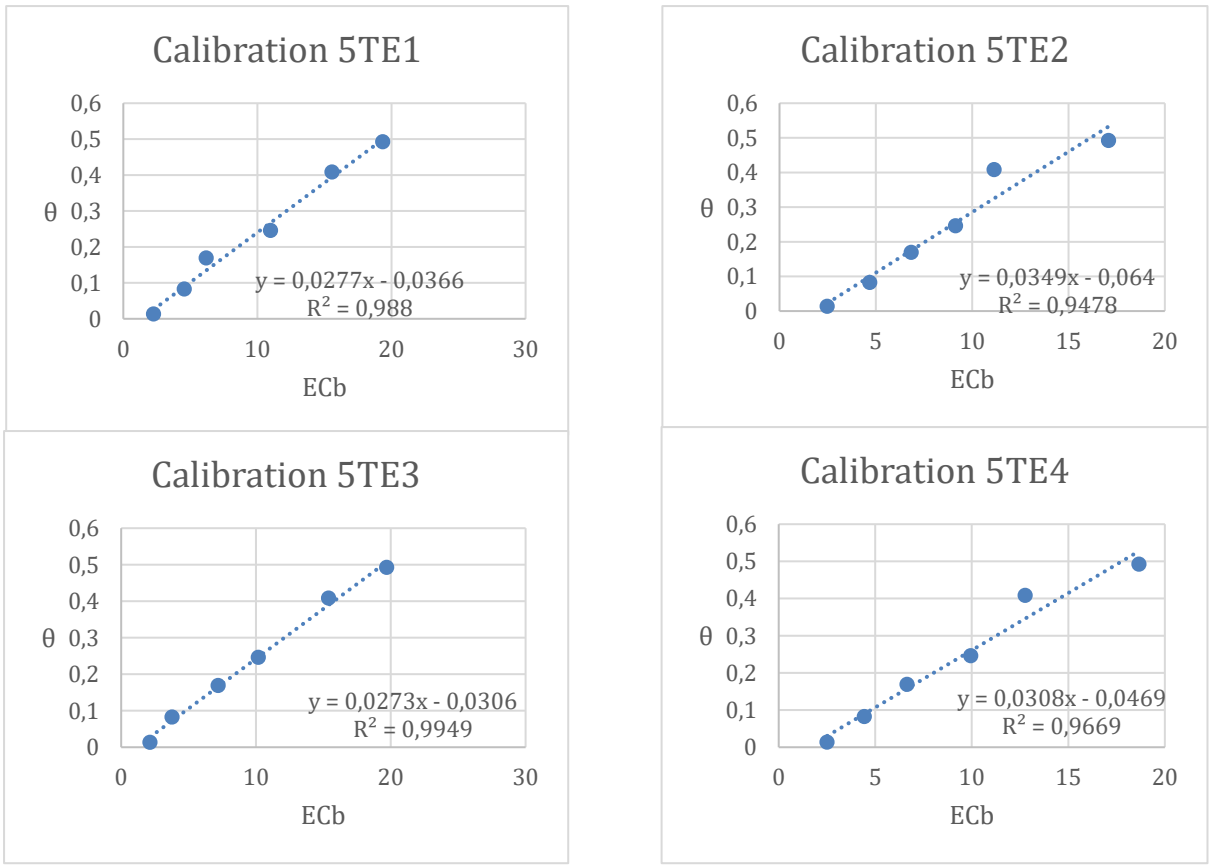

Figure D-2: 5TE calibration equation

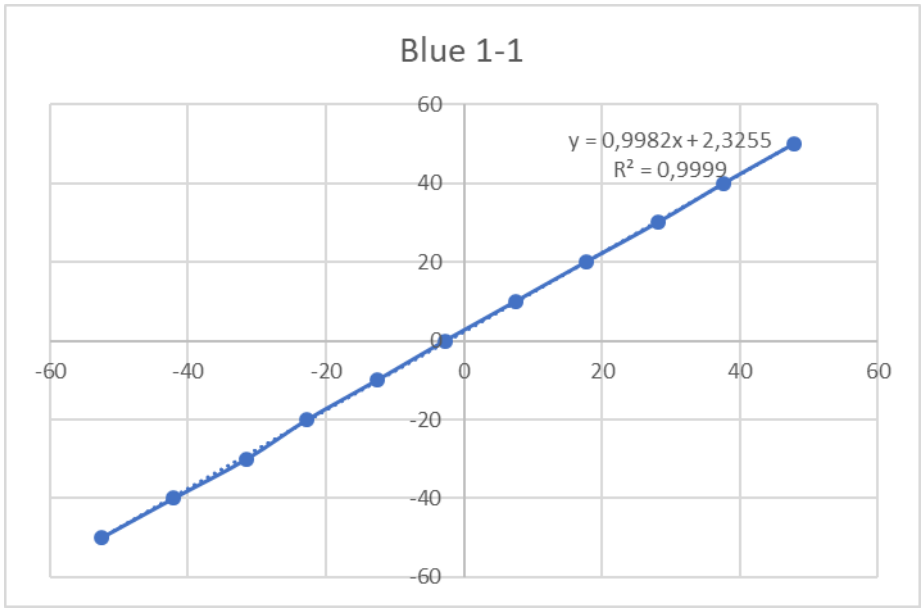

Figure D-3: Calibration curve tensio 1

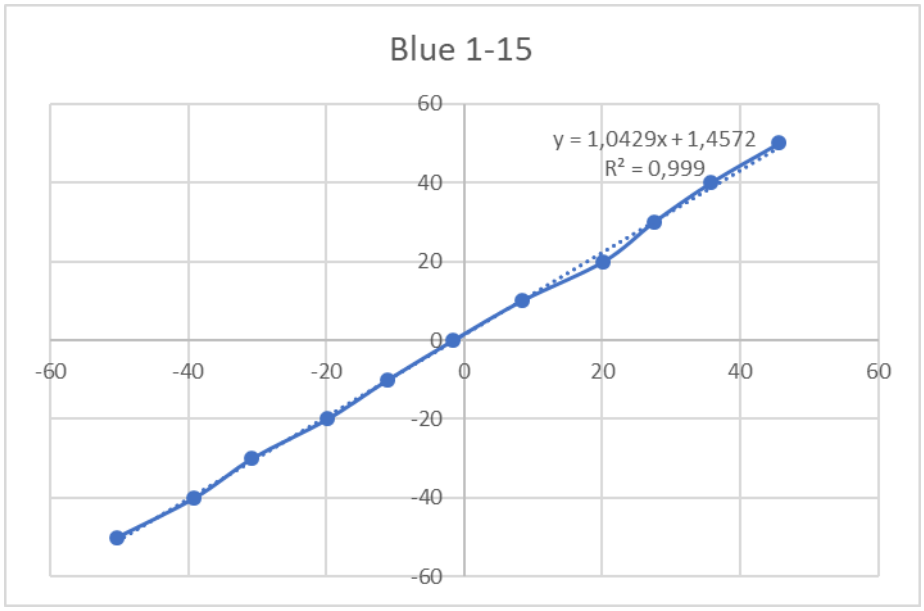

Figure D-4: Calibration curve tensio 2

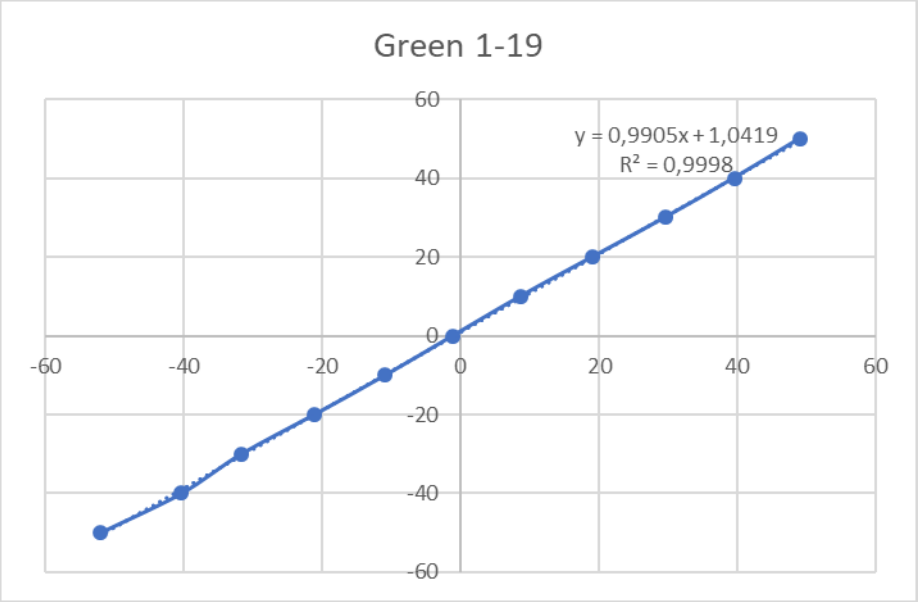

Figure D-5: Calibration curve tensio 3

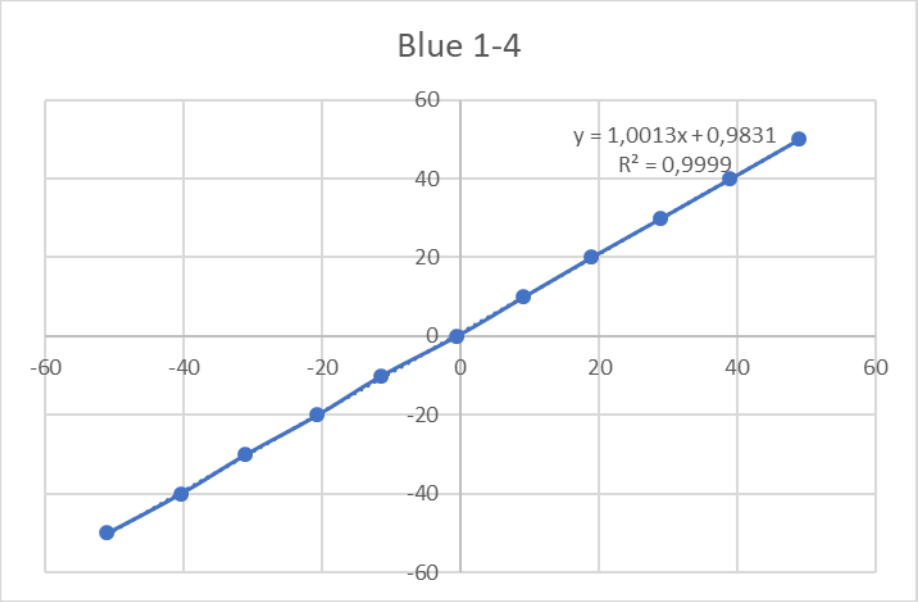

Figure D-6: Calibration curve tensio 4

E. Data logging

CR1000X

Figure E-1 CR1000X data logger

Data logger program

'CR1000X Series Datalogger

'--

'By: Harm Gooren, WageningenUR

'File: Colomns Mojtaba v01.CR1

'Date: August 3th, 2015

'Subject: For column experiment with 3 tensiometers, 3x Decagon 5TE and 4-wire salinity probe

'--

'revision 01: August 4th, 2015: First setup (GCv20 for 5TE's)

'revision 02: September 25th, 2015: Change conductivity measurements for Consort R315

'revision 03: November 11th, 2016: Changed convertion ds/m to us/cm

'revision 04: November 25th, 2016: Changed the dielectric permittivity of the dry soil to 3 (from 6) and changed storage interval to 30 seconds (from 1 minute)

'revision 05: September 17th, 2020: Changed to CR1000X and for 4 sets of sensors (5TE and Tensiometer)

'--

Public Tensio(4) 'Matric head measured by Tensiometers

'Public Conduc 'Conductivity from Consort R315

Units Tensio=cmH2O 'Matric head in cm watercolumn

```
Public PTemp, batt_volt

'=====For TE5 sensors
Public TE5(4,3)
Const eb0 = 3                    'empirical constant loosely representing the dielectric of dry soil

Public VWCm5TE(4) As Float 'VWCp5TE(8) As Float // VWCm for mineral soil, VWCp for potting soil
Public Temp5TE(4) As Float
Public Eb5TE(4) As Float, ep5TE(8) As Float 'Eb is bulk dielectric and ep is the dielectric of the pore water
Public ECb5TE(4) As Float ' this is bulk dielectric measured by the 5TE
Public ECp5TE(4) As Float ' this is the pore water dielectric estimated by Hilhorst (2000)
Public i As Float
Units VWCm5TE=m^3/m^3
'Units VWCp5TE=m^3/m^3
Units Temp5TE=degC
Units ECb5TE=uS/cm      'Bulk electrical conductivity uS/cm; note that original program was in dS/m or mS/cm!!!
Units ECp5TE=uS/cm      'Pore electrical conductivity uS/cm; note that original program was in dS/m or mS/cm!!!


'=====

'Storage of the data in a table:
DataTable (ColumnData,1,-1)
  DataInterval (0,5,Min,0)              'Interval is second and third parameter of this command,
  'change as desired (as long as it is a multiple of the scan interval)
  Sample (1,PTemp,FP2)                          'Internal temperature of the CR1000
  Sample (1,batt_volt,FP2)                  'Supply voltage
  Sample (4,Eb5TE(),FP2)                'Eb is bulk dielectric and ep is the dielectric of the pore water
  Sample (4,VWCm5TE(),FP2)                  'Volumetric Water Content measured by 5TE sensors
  Sample (4,ECb5TE(),IEEE4)                 'Bulk electrical conductivity uS/cm; note that original program was in dS/m or mS/cm!!!
```

```
 Sample (4,ECp5TE(),IEEE4)                    'Pore electrical conductivity uS/cm; note that original program was in dS/m or mS/cm!!!
 Sample (4,Temp5TE(),FP2)                     'Temperature measured by 5TE sensors
 Sample (4,Tensio(),FP2)                      'Matric head measured by Tensiometers

EndTable

SequentialMode                                                    'VERY IMPORTANT TO RUN THIS PROGRAM IN SEQUENTIAL MODE!!!

'Main Program
'================================================================================================================

BeginProg
 Scan (5,Sec,0,0)                                                 'Scan interval should NOT be shorter than 5 seconds, time needed to measure all sensors!!
  PanelTemp (PTemp,_50Hz)                                         'Internal temperature of the CR1000; gives an indication of the room temperature.
  Battery (batt_volt)                                             'Check if the power supply is OK (between 9.6 and 16 Volt DC)

  SW12 (SW12_2,1 )'supply power to all 5TE sensors by SW12_2 port
  Delay (0,2,Sec)

  'To measure TE5 sensor 1 on Control Port 1
  i=1
  SDI12Recorder (TE5(i,1),C1,0,"M!",1.0,0)
      'Returns three values for each sensor: Temp ~ [–40, +60] °C; εb ~ 1 (air) to 80 (water); ECb: [0–23] dS/m (bulk);
  Temp5TE(i) = TE5(i,3)
      'Temperature (sensor);
  Eb5TE(i) = TE5(i,1)
      'εa = Soil bulk dielectric permitivity (sensor);
  VWCm5TE(i) = 4.3E-6 * TE5(i,1)^3 - 5.5E-4 * TE5(i,1)^2 + 2.92E-2 * TE5(i,1) - 5.3E-2
      'VWC= Volumetric water content from Topp et al. (1980)
```

```
  ECb5TE(i) = TE5(i,2)*1000
        'ECb= Bulk Electrical Conductivity,*1000 dS/m to uS/cm;
  ep5TE(i) = 80.3 - 0.37*(Temp5TE(i)- 20)
        'εp =  Dielectric permittivity of the soil pore water in uS/cm;
  If Eb5TE(i) > 3 Then
   ECp5TE(i) = (ep5TE(i)*ECb5TE(i))/(Eb5TE(i)-eb0)
        'Hilhorst (2000), pore water EC in uS/cm; note that original program used ECbTE5 1000 times smaller to get dS/m or mS/cm!!!
  Else
   ECp5TE(i) = ECb5TE(i)
        'If εp<3 => pore water EC = Bulk EC, because VWC < 0.10, (Eb5TE(i)-eb0)~0.
  EndIf

'To measure TE5 sensor 2 on Control Port 3
  i=2
  SDI12Recorder (TE5(i,1),C3,0,"M!",1.0,0)          'Returns three values for each sensor.
  Temp5TE(i) = TE5(i,3)
  Eb5TE(i) = TE5(i,1)
  VWCm5TE(i) = 4.3E-6 * TE5(i,1)^3 - 5.5E-4 * TE5(i,1)^2 + 2.92E-2 * TE5(i,1) - 5.3E-2' Topp et al. (1980)
  ECb5TE(i) = TE5(i,2)*1000 'Bulk Electrical Conductivity from dS/m to uS/cm;
  ep5TE(i) = 80.3 - 0.37*(Temp5TE(i)- 20)
  If Eb5TE(i) > 3 Then
   ECp5TE(i) = (ep5TE(i)*ECb5TE(i))/(Eb5TE(i)-eb0)                    'Pore EC in uS/cm; note that original program used ECbTE5 1000 times smaller to get dS/m or mS/cm!!!
  Else
   ECp5TE(i) = ECb5TE(i)
  EndIf

'To measure TE5 sensor 3 on Control Port 5
  i=3
  SDI12Recorder (TE5(i,1),C5,0,"M!",1.0,0)          'Returns three values for each sensor.
  Temp5TE(i) = TE5(i,3)
  Eb5TE(i) = TE5(i,1)
  VWCm5TE(i) = 4.3E-6 * TE5(i,1)^3 - 5.5E-4 * TE5(i,1)^2 + 2.92E-2 * TE5(i,1) - 5.3E-2' Topp et al. (1980)
  ECb5TE(i) = TE5(i,2)*1000 'Bulk Electrical Conductivity from dS/m to uS/cm;
```

```
  ep5TE(i) = 80.3 - 0.37*(Temp5TE(i)- 20)
  If Eb5TE(i) > 3 Then
   ECp5TE(i) = (ep5TE(i)*ECb5TE(i))/(Eb5TE(i)-eb0)                    'Pore EC in uS/cm; note that original program used ECbTE5 1000 times smaller to get dS/m or mS/cm!!!
  Else
   ECp5TE(i) = ECb5TE(i)
  EndIf

'To measure TE5 sensor 4 on Control Port 7
  i=4
  SDI12Recorder (TE5(i,1),C7,0,"M!",1.0,0)          'Returns three values for each sensor.
  Temp5TE(i) = TE5(i,3)
  Eb5TE(i) = TE5(i,1)
  VWCm5TE(i) = 4.3E-6 * TE5(i,1)^3 - 5.5E-4 * TE5(i,1)^2 + 2.92E-2 * TE5(i,1) - 5.3E-2' Topp et al. (1980)
  ECb5TE(i) = TE5(i,2)*1000 'Bulk Electrical Conductivity from dS/m to uS/cm;
  ep5TE(i) = 80.3 - 0.37*(Temp5TE(i)- 20)
  If Eb5TE(i) > 3 Then
   ECp5TE(i) = (ep5TE(i)*ECb5TE(i))/(Eb5TE(i)-eb0)                    'Pore EC in uS/cm; note that original program used ECbTE5 1000 times smaller to get dS/m or mS/cm!!!
  Else
   ECp5TE(i) = ECb5TE(i)
  EndIf


  SW12 (SW12_2,0) 'Switch off the power for the 5TE sensors


'Generic Full Bridge measurement Conductivity by the 4 wire salinity Probe:
  'BrFull(Conduc,1,mV2500,3,Vx1,1,2500,True,True,0,_50Hz,1.0,0.0)

  'Convert 4-20mA signal from Consort R315 to uS/cm. V=I*R, R = 100 Ohm, 4mA*100=400mV = 0uS/cm, 20mA*100=2000mV = 20000uS/cm. (2000-400)/20000=0.08, 0.08*400=32
  'Convert 4-20mA signal from Consort R315 to uS/cm. V=I*R, R = 100 Ohm, 398.6mV = 0uS/cm, 574.56mV = 2190uS/cm. = 12.446, 12.446*398.6=4960.98
```

'VoltDiff(Conduc,1,mV2500,1,True,0,_50Hz,12.603,-5063.62)

'VoltDiff(Conduc,1,mV2500,1,True,0,_50Hz,1,0)

'Measurements of the Pressure in the tensiometers on diff channels 6 to 8

BrFull(Tensio(1),1,mV200,2,Vx1,1,2000,True,True,30000,_50Hz,276.25,-1) '276.25 is a multiplier that should be close to correct (I use 277 often), -1 is an offset in cmH2O, that should be checked for each sensor.

BrFull(Tensio(2),1,mV200,3,Vx2,1,2000,True,True,30000,_50Hz,276.25,-1)

BrFull(Tensio(3),1,mV200,6,Vx3,1,2000,True,True,30000,_50Hz,276.25,-1)

BrFull(Tensio(4),1,mV200,7,Vx4,1,2000,True,True,30000,_50Hz,276.25,-1)

CallTable (ColumnData)

NextScan

EndProg

3. SYSTEM

This section describes the 5TE sensor.

3.1 SPECIFICATIONS

MEASUREMENT SPECIFICATIONS	
Volumetric Water Content (VWC)	
Range	
Mineral soil calibration	0.0–1.0 m^3/m^3
Soilless media calibration	0.0–1.0 m^3/m^3
Apparent dielectric permittivity (ε_a)	1 (air) to 80 (water)
Resolution	0.0008 m^3/m^3 from 0%–50% VWC
Accuracy	
Generic calibration	± 0.03 m^3/m^3 typical
Medium-specific calibration	±0.02 m^3/m^3
Apparent dielectric permittivity (ε_a)	1–40 (soil range), ±1 ε_a (unitless) 40–80, 15% measurement
Temperature	
Range	–40 to +60 °C
Resolution	0.1 °C
Accuracy	±1 °C
Bulk Electrical Conductivity (EC)	
Range	0–23 dS/m (bulk)
Resolution	0.01 dS/m from 0–7 dS/m 0.05 dS/m from 7–23 dS/m
Accuracy	±10% from 0–7 dS/m User calibration required from 7–23 dS/m

COMMUNICATION SPECIFICATIONS

Output
DDI serial or SDI-12 communication protocol
Data Logger Compatibility
Data acquisition systems capable of 3.6- to 15.0-VDC power and serial or SDI-12 communication

PHYSICAL SPECIFICATIONS

Dimensions	
Length	10.9 cm (4.3 in)
Width	3.4 cm (1.3 in)
Height	1.0 cm (0.4 in)

Prong Length
5.0 cm (1.9 in)

Operating Temperature Range	
Minimum	–40 °C
Typical	NA
Maximum	+60 °C

NOTE: Sensors may be used at higher temperatures under certain conditions; contact Customer Support for assistance.

Cable Length
5 m (standard) 75 m (maximum custom cable length)

NOTE: Contact Customer Support if a nonstandard cable length is needed.

Connector Types
3.5-mm stereo plug connector or stripped and tinned wires

ELECTRICAL AND TIMING CHARACTERISTICS

Supply Voltage (VCC to GND)	
Minimum	3.6 VDC
Typical	NA
Maximum	15.0 VDC

Digital Input Voltage (logic high)	
Minimum	2.8 V
Typical	3.0 V
Maximum	3.9 V
Digital Input Voltage (logic low)	
Minimum	–0.3 V
Typical	0.0 V
Maximum	0.8 V
Power Line Slew Rate	
Minimum	1.0 V/ms
Typical	NA
Maximum	NA
Current Drain (during measurement)	
Minimum	0.5 mA
Typical	3.0 mA
Maximum	10.0 mA
Current Drain (while asleep)	
Minimum	NA
Typical	0.03 mA
Maximum	NA
Power-Up Time (DDI serial)	
Minimum	NA
Typical	NA
Maximum	100 ms
Power-Up Time (SDI-12)	
Minimum	100 ms
Typical	150 ms
Maximum	200 ms

Measurement Duration	
Minimum	NA
Typical	150 ms
Maximum	200 ms

COMPLIANCE

Manufactured under ISO 9001:2015
EM ISO/IEC 17050:2010 (CE Mark)

3.2 ABOUT 5TE

The 5TE is designed to measure the water content, EC, and temperature of soil (Figure 5). The 5TE uses an oscillator running at 70 MHz to measure the dielectric permittivity of soil to determine the water content. A thermistor in thermal contact with the sensor prongs provides the soil temperature, while the screws on the surface of the sensor form a two-sensor electrical array to measure EC. The polyurethane coating on the 5TE circuit board protects the components from water damage and gives the sensor a longer life span.

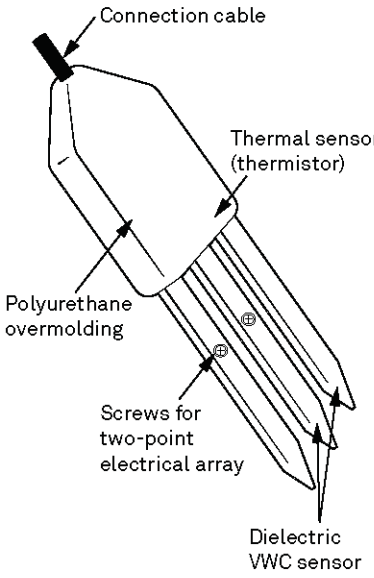

Figure 5 5TE components

F. Nutrolase datasheet

AVEBE SPECIALTIES

P.O. Box 15
9640 AA Veendam
The Netherlands
CustomerService@AVEBE.COM
WWW.AVEBE.COM

NUTROLASE™

Nutrients for soil remediation

NUTROLASE™ is a blend of nutrients for in-situ soil remediation. NUTROLASE™ stimulates natural attenuation by providing a feedstock to micro-organisms that can dehalogenate carbohydrates such as Dehalococcoides Ethenogenes.
Under anaerobic conditions NUTROLASE™ acts as electron donor. It favours the creation of optimal circumstances for dehalogenation by lowering the redox potential of the soil.
In many reported cases the stimulated growth of micro-organisms has lead to a relatively fast and complete conversion of volatile organic chlorinated carbohydrate (VOCL) type pollutants into harmless molecules.
NUTROLASE™ has been successfully applied on many polluted sites.

NUTROLASE™ is available as a viscous liquid that can be introduced into the polluted area by direct injection or by injection through drains.

Product description

- Nature: Viscous solution
- Appearance: Brown liquor
- Bulk density: 1200 kg/m^3
- Moisture content: 440 mg/g
- Compatibility: Compatible with other nutrients
- TOC (Total Organic Carbon): 200 g/l

Composition

NUTROLASE™ is a complex source of carbon. An indication of the composition is presented below:

Component	Indicative amount (g/kg)
Water	440
Cations	85
Anions	50
Acids	126
Sugars	87
Proteins	190
Others	23
Total	1000

Main Applications

NUTROLASE™ has been successfully applied to sites polluted by various halogens such as:
- Tetrachloro-ethene (PER)
- Di, tri and monochloroethene
- Trichloroethane (TRI)
- Dichloroethane

Advantages

- NUTROLASE™ contains a blend of organic acids, sugars, proteins and amino acids and a various salts including potassium and phosphates.
- NUTROLASE™ favours the creation of the optimal circumstances for dehalogenation of VOCL.
- Use of NUTROLASE™ leads to complete remediation of the pollutants.

Product Information

ref.no. 119746/version 03, issued May 01, 2012, valid till May 01, 2015

NUTROLASE™

Directions for use

It is recommended to study the efficacy of NUTROLASE™ prior to the remediation by lab experiments and / or a pilot study. The time needed for remediation depends on the specific conditions in the target area such as soil composition, temperature, pH etc. and type of solution. NUTROLASE™ contains a small amount of solids which can cause plugging, e.g. of remediation drains. It is recommended to sieve NUTROLASE™ prior to use.
NUTROLASE™ can be diluted to the required concentration upon use. The optimal dosage is depending on the way of application and the type of use. Addition is usually in the following range:

• Dilute 1 part of NUTROLASE™ with 100 parts of water.

Packing and Storage

NUTROLASE™ is available in IBC - intermediate bulk containers (1000 litre).

Technical service

Complete details for every use are difficult to cover adequately in this brochure because of varying local conditions. The technical staff of the AVEBE will gladly supply any further particulars about recipes to achieve optimum results in your specific application.

ref.no. 119746/version 03, issued May 01, 2012, valid till May 01, 2015